energies

MDPI

Article

Evaluating the Use of Displacement Ventilation for Providing Space Heating in Unoccupied Periods Using Laboratory Experiments, Field Tests and Numerical Simulations

Saqib Javed [1,*], Ivar Rognhaug Ørnes [2], Tor Helge Dokka [2], Maria Myrup [2] and Sverre Bjørn Holøs [3]

[1] Building Services, Lund University, 221 00 Lund, Sweden
[2] Climate, Energy and Building Physics, Skanska Norway, 0107 Oslo, Norway; ivar.ornes@skanska.no (I.R.Ø.); Tor.helge.dokka@skanska.no (T.H.D.); maria.myrup@skanska.no (M.M.)
[3] Architectural Engineering, SINTEF Community, 0373 Oslo, Norway; SverreB.Holos@sintef.no
* Correspondence: saqib.javed@hvac.lth.se; Tel.: +46-46-222-1745

Abstract: Displacement ventilation is a proven method of providing conditioned air to enclosed spaces with the aim to deliver good air quality and thermal comfort while reducing the amount of energy required to operate the system. Until now, the practical applications of displacement ventilation have been exclusive to providing ventilation and cooling to large open spaces with high ceilings. The provision of heating through displacement ventilation has traditionally been discouraged, out of concern that warm air supplied at the floor level would rise straight to the ceiling level without providing heat to the occupied space. Hence, a separate heating system is regularly integrated with the displacement ventilation in cold climates, increasing the cost and energy use of the system. This paper goes beyond the common industry practice and explores the possibility of using displacement ventilation to provide heating without any additional heating system. It reports on experimental investigations conducted in laboratory and field settings, and numerical simulation of these studies, all aimed at investigating the application of displacement ventilation for providing a comfortable indoor environment in winter by preheating the space prior to occupancy. The experimental results confirm that the proposed concept of providing space heating in unoccupied periods without a separate heating system is possible with displacement ventilation.

Keywords: indoor air quality; thermal comfort; CO_2 concentrations; classroom; preheating; stratification

Citation: Javed, S.; Ørnes, I.R.; Dokka, T.H.; Myrup, M.; Holøs, S.B. Evaluating the Use of Displacement Ventilation for Providing Space Heating in Unoccupied Periods Using Laboratory Experiments, Field Tests and Numerical Simulations. *Energies* **2021**, *14*, 952. https://doi.org/10.3390/en14040952

Academic Editor: John Kaiser Calautit

Received: 16 January 2021
Accepted: 5 February 2021
Published: 11 February 2021

1. Introduction

In modern societies, people are spending increasingly more time in indoor environments. Due to the wide spectrum of pollutants and contaminants present in these confined environments, indoor air quality (IAQ) has become a matter of great importance [1]. It has been repeatedly and conclusively demonstrated that indoor air quality has a significant influence on human health, comfort, and productivity [2,3]. The most common method for controlling and improving indoor air quality is the dilution of indoor pollutants and contaminants by providing clean air through ventilation. It is well-established that a higher ventilation rate, i.e., bringing in more fresh outdoor air, is advantageous for reducing indoor air pollutants and thus achieving better indoor air quality [4]. However, improving indoor air quality by increasing ventilation rates is directly correlated with increased energy use in buildings [5]. Today, the energy demands of newly constructed and renovated buildings are tightly controlled through legislative building regulations and codes. Furthermore, voluntary building certification programs like BREEAM (Building Research Establishment Environmental Assessment Method) [6] and LEED (Leadership in Energy and Environmental Design) [7] also require buildings to reduce their energy consumption. In order to fulfil the somewhat contradictory requirements of providing high indoor air quality while simultaneously satisfying the requirements of low energy consumption, displacement ven-

tilation has, in recent years, emerged as an efficient and a superior alternative to the more commonly used mixing ventilation.

Figure 1 presents a conceptual illustration of the most salient aspects of displacement ventilation. In displacement ventilation, relatively cold, and thus heavier air is supplied to space at low levels. The cold air is warmed up by heat sources present in the space, including, for example, people, lighting and equipment, etc. The air moves upwards as thermal plumes due to buoyancy effects induced by density differences. The ascending thermal plumes reach the equilibrium density level at the so-called stratification height, after which they spread horizontally. The warm and lighter air is thus accumulated below the ceiling level and is extracted from the space at high levels. The thickness of the upper layer depends upon the plume and the supply airflows. The pollutants and contaminants that are either warmer and/or lighter than the surrounding air are also led upward by the ascending displacement flow. Wherefore the ventilated space becomes divided into two zones: A lower occupied zone with clean air and an upper unoccupied zone with contaminated air. In order to provide the same level of ventilation, displacement ventilation requires considerably lower volume flows than the more commonly used mixing ventilation. This is because the air distribution effectiveness of displacement ventilation systems is significantly higher than that of mixed ventilation systems [8]. This, in turn, means lower energy consumption by fans as well as reduced energy consumption for thermal conditioning of the ventilation air.

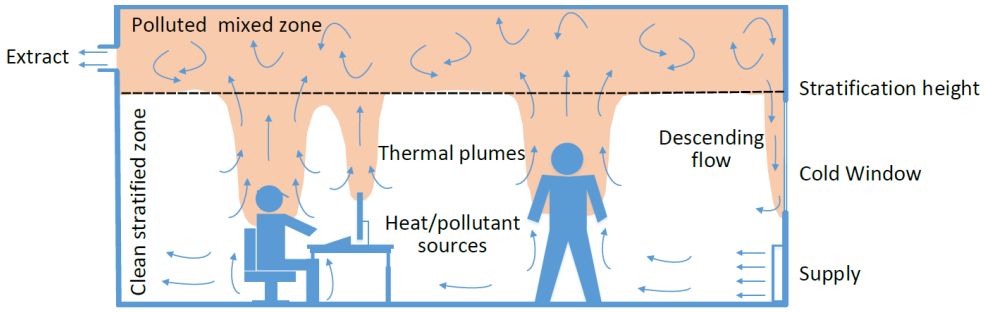

Figure 1. Illustration of displacement ventilation.

The supply air may quickly rise from the occupied zone to the unoccupied zone if its temperature is too close or higher than the room temperature. In such a case, the effectiveness of the displacement ventilation may well be reduced significantly due to the short-circuiting of the supply air. Since the supply air in displacement ventilation is provided at a temperature lower than the space temperature, the applications of displacement ventilation have largely been confined to providing ventilation and cooling to the conditioned spaces. Sometimes, displacement ventilation is also used together with radiant cooling systems, e.g., chilled ceilings, and floor cooling. However, the provision of heating through the displacement ventilation has generally been discouraged because of the potential short-circuiting of the warm buoyant air to the unoccupied zone [9]. The use of an auxiliary heating system, e.g., floor heating, ceiling panels, and wall radiators and convectors, has been recommended for space heating when using displacement ventilation [10]. Using a separate heating system not only inflates the capital and operating costs of the overall system [11], but also leads to increased environmental impacts due to higher material and energy use [12].

This paper is based on the hypothesis that displacement ventilation can be used for providing space heating, primarily to avoid the added cost and environmental impacts of a separate heating system. A few exploratory studies [13,14] have shown that there may exist more potential for heating with displacement ventilation using slightly elevated supply temperatures than hitherto suggested in the literature. If the extraction and supply points are carefully located to avoid short-circuiting, e.g., at opposite ends of the room, supplying warm air through the displacement ventilation system destroys the vertical stratification in

the space and results in mixing ventilation like air distribution [15]. Elsewise, special displacement diffusers with integrated heating sections, supplying slow-moving cold air for cooling from one part and fast-moving warm air for heating from the other part, may be used [16]. Another possible approach is to provide heating outside the occupied hours through the ventilation system. This way, space can be preheated to a suitable temperature level by supplying warm air during the non-occupancy periods, e.g., at night. In the occupied hours, space can then be provided with normal displacement ventilation, i.e., supplying air with a temperature a few degrees below the room temperature.

The objective of this paper is to increase understanding of the application of displacement ventilation systems for providing heating through supply air, without any separate heating system. This is accomplished through a field test in a real classroom environment, laboratory tests on a scaled model of a classroom, and simulation studies of these tests. The paper first provides an extensive review of literature on the use of displacement ventilation. It then presents a field application of displacement ventilation providing night-time heating. The paper next describes the methodology of the field and the laboratory tests, and the simulation study, followed by the results from these investigations. A comparative discussion of the experimental and simulation results is then presented, together with design recommendations and lessons learned for practitioners and researchers interested in applying displacement ventilation with night-time heating. Finally, conclusions and final remarks are presented.

2. Literature Review

Displacement ventilation has been extensively studied in the literature. Several reference manuals and design guides [9,17–19] offering a detailed description of design procedures and methods, design strategies and constraints, technical and performance requirements, and application examples and case studies of displacement ventilation, have been published.

The typical installations of displacement ventilation include meeting rooms, lecture halls, auditoriums, theaters, conference rooms, shopping malls, and atriums, among others. One common application of displacement ventilation systems, also considered in this study, is in classrooms and school buildings, where indoor air quality and thermal comfort are of great significance due to their impact on both the learning environment and on students' health and wellness. Schools have considerably higher occupancy densities than office buildings, which, in turn, results in higher internal gains and larger concentrations of indoor pollutants. Several studies, including [20–23], have noted that indoor air quality and thermal comfort problems are widespread in schools and other educational buildings. Ventilation rates are often inadequate in classrooms [24] and microbiological contaminants (e.g., allergens, fungi, and bacteria), formaldehyde, and total volatile organic compounds are commonly found in school and classroom environments [25]. Displacement ventilation is often used in classrooms and schools to provide a high level of air quality. Compared to mixing ventilation, displacement ventilation has been shown to result in lower concentrations of pollutants and contaminants in classrooms, at least in the breathing zone, and to improve the overall perception of air quality among students [26]. Moreover, displacement ventilation has also been shown to yield significant energy savings in schools [27].

Modeling for the design and simulation of displacement ventilation systems has been an open research topic. The most commonly used modeling approach for sizing displacement ventilation systems for non-industrial applications is the so-called temperature-based design approach. In this approach, the supply airflow and the supply air temperature are determined based on the heat balance of the occupied and upper zones in the room [9]. As stratification in the occupied zone is important for the thermal comfort of the occupants, the approach involves a calculation of the vertical air temperature gradient in the room using a temperature stratification model, such as those suggested presented by Mundt [28], Nielsen [29], or Mateus and da Graça [30], among others. These models differ in their assumptions about the temperature distribution in the room, and the number of temper-

ature nodes used to model the temperature profile. The Mundt model assumes a linear distribution of the indoor air temperature over the entire room height. The temperature profile of the room air is obtained using two temperature nodes, one at the floor level and the other at the ceiling level. The convective heat transfer from the floor surface to the supply air is taken equal to the radiative heat exchange between the ceiling and the floor surfaces. This model has been implemented in some building energy simulation software, such as EnergyPlus [31] and IDA Indoor Climate and Energy (IDA-ICE) [32]. The Nielsen model also considers a linear temperature distribution of indoor air but, unlike the Mundt model, the temperature gradient is only considered linear between the floor level and the stratification height, above which the air temperature is taken to be constant. The model calculates the vertical air temperature gradient based on the so-called Archimedes number of the flow and the type of heat source in the occupied zone. The Mateus and da Graça model considers a non-linear temperature distribution in the room. The model predicts the temperature profile of the indoor air using three temperature nodes, one at the floor level, one in the occupied zone, and one at the stratification height. Above the stratification height, the air temperature is considered constant by the model. The model considers four room surfaces, i.e., floor, ceiling, and two lateral wall portions. The radiative heat exchange between these surfaces and the convective heat exchange between each room surface and the corresponding air temperature node connected to it is accounted for by the model. The entrainment generated accumulated flows and the convective heat gains that get mixed into the occupied zone, and, are not directly carried to the stratification height are also considered by the model.

A more complicated and consequently less used, modeling approach for sizing displacement ventilation systems is the so-called shift zone design approach. In this approach, the supply airflow at the stratification height, taken above the breathing zone, is set equal to the total upwards convective flows. The supply airflow is chosen to ensure that the contamination concentrations are below the threshold levels in the occupied zone and that the thermal comfort conditions in the occupied zone are met. Hence, in the shift zone approach, in addition to the modeling temperature gradient in the room, modeling contaminant concentration gradients are equally desirable. Calculation of the vertical contaminant gradient is generally carried out using zonal models, such as those proposed by Skåret [33], Koganei et al., [34], Sandberg et al., [35] Dokka [36], or Yamanaka [37], among others.

Factors affecting the design and performance of displacement ventilation have been extensively studied using simulations, experiments, and field tests. Several laboratory and field studies have been undertaken to examine the underlying principles of thermal stratification and contaminant dilution. Okutan et al., [38] investigated the performance of displacement ventilation systems in open-plan office environments using a scale model, focusing in particular on vertical temperature distribution. Brohus and Nielsen [39] examined the effects of persons present in a displacement ventilated room on the contaminant distribution through full-scale measurements. In another study, the authors also probed the exposure of a seated and a standing person in proportion to the stratification height [40]. Akimoto et al., [41] studied the indoor thermal environment of the floor-supply displacement ventilation system in a controlled chamber altering the supply air volume, heat load, and position of heat sources. Yuan et al., [42,43] performed detailed measurements on the age of air and the vertical profiles of air temperature, air velocity, and contaminant concentration in a test chamber with displacement ventilation, simulating a small office, a large office with partitions, and a classroom. Xu et al., [44,45] examined the effect of heat loss through walls upon the distribution of temperature and contaminant concentration in an experimental room with displacement ventilation. Mundt [46] evaluated particle transportation and ventilation efficiency in a displacement-ventilated room with non-buoyant pollutant sources. Cheong et al., [47,48] assessed the effects of local and overall thermal sensations and comfort in a field environmental chamber served by a displacement ventilation system. Wachenfeldt et al., [49] evaluated the airflow rates and energy-saving potential of demand-controlled displacement ventilation systems in two

Norwegian schools. Trzeciakiewicz [50] investigated the two-zone airflow patterns and determined the stratification heights in a mock-up office room under conditions of various heat sources and airflow rates. Yu et al., [51] investigated the thermal influence of temperature gradient on overall and local thermal comfort at different room air temperatures in a large environment chamber served by displacement ventilation. These studies suggest that several factors are key to the design and performance of displacement ventilation systems, and thus must be considered in both modeling and experimental analysis of these systems.

The effects of supply air conditions, heat and contaminant sources, and other practical issues concerning displacement ventilation have also been assessed using computer simulations. Lin et al., [52,53] and Kang et al., [54] examined the effects of supply air temperature and supply air location on the performance of displacement ventilation using CFD (computational fluid dynamics) analysis. Yuan et al., [43], Kobayashi and Chen [55], and Lin and Lin [56] studied the influence of supply airflow. Mathisen [57], Zhang et al., [58], and Cehlin and Moshfegh [59] reported on the effects of supply air diffuser on displacement ventilation. Several researchers including Park and Holland [60], Rees et al., [61], Deevy et al. [62], Zhong et al. [63], and Causone et al. [10] probed the effect of the heat and contaminant source location on the displacement ventilation performance using CFD simulations. Matsumoto et al., [64], Matsumoto and Ohba [65], and Mazumdar et al. [66] studied the impact of moving sources on the displacement ventilation. Li et al., [67], Faure and Le Roux [68], and Wu et al., [69] investigated the effects of heat losses, gains, and transfers from different room-envelope elements on the distribution of temperature and contaminant concentration in rooms with displacement ventilation. Lin et al., [70], and Hashimoto and Yoneda [71] studied the influence of ceiling height on the performance of the displacement ventilation. Lin et al., [72] and Mazumdar et al., [66] explored the impact of the door opening on thermal and contaminant distribution in the room through computer simulations. The results of the simulation studies indicate that supply air conditions, heat and contaminant source characteristics, envelope properties, and movements in the space all have a profound impact on displacement ventilation.

Some experimental studies have examined air terminal and air-jet characteristics for displacement ventilation under a variety of supply air and indoor conditions. Xing et al. [73] tested three different types of displacement diffusers, including a flat-wall diffuser, a semi-circular diffuser, and a floor swirl diffuser, and measured the age of air distribution, air exchange index, and ventilation effectiveness for each diffuser type in a mock-up office room with varying thermal loads. In a related study, Xing and Awbi [74] assessed the relationship between stratification height and ventilation load under similar experimental settings. Kobayashi and Chen [55], and Lau and Chen [75] studied the performance of floor supply displacement ventilation system in a full-scale environmental chamber, simulating a two-person office room with swirl diffusers and a workshop with perforated panels and swirl diffusers, respectively. Fatemi et al., [76] analyzed the flow physics of a non-isothermal jet stream in a large room supplied by a relatively large corner-mounted quarter-round displacement diffuser. Fernández-Gutiérrez et al., [77] characterized a small-scale, low-velocity displacement diffuser in a laboratory test chamber through flow visualizations and velocity field measurements. Magnier [78] investigated velocity and temperature distribution in air jets from two different wall-mounted displacement ventilation diffusers, for different supply conditions. The experimental studies show that the effectiveness of the displacement ventilation system is directly affected by the type of the diffuser and characteristics of the supply air jet.

A few studies have experimentally investigated the combination of displacement ventilation with radiant heating and cooling systems. Causone et al., [79] experimentally evaluated the possibilities and limitations of combining radiant floor heating and cooling with displacement ventilation. The profiles of air temperature, velocity and ventilation effectiveness were measured under typical office conditions. Wu et al., [69] investigated the air distribution and ventilation effectiveness of displacement ventilation systems with floor heating and ceiling heating systems in a laboratory investigation. Rees and Haves [80]

studied airflow and temperature distribution in a test chamber with displacement ventilation and a chilled ceiling over a range of operating parameters typical of office applications. Schiavon et al., [81] performed laboratory experiments to study the room air stratification and air change effectiveness in a typical office space with a combined radiant chilled ceiling and displacement ventilation system. All these studies indicate that radiant systems for supplemental heating and cooling are well-suited for displacement ventilation. In a particularly unique series of field studies in three Canadian schools, Ouazia et al., [14,82] evaluated the performance of displacement ventilation in heating mode with supplementary perimeter heating systems. The contaminant removal effectiveness of the displacement ventilation in the heating mode was found to be higher than previously suggested in the literature. Moreover, thermal comfort indices, including vertical temperature gradient and draft ratio, were also found to be satisfactory.

Several studies have focused on comparing the performance characteristics of displacement ventilation with mixing ventilation. Akimoto et al., [83] and Rimmer et al., [84] compared the two ventilation systems in terms of the mean age of the air in an environmental chamber simulating an office room, and an actual hospital building, respectively. Breum [85] studied the displacement and mixing ventilation systems in terms of exposure to a simulated body odor in an experimental chamber. Olmedo et al., [86] investigated the human exhalation flows for the two systems in a full-scale test chamber. Wu et al., [87] explored air distribution for the two systems with or without floor and ceiling heating in a multi-occupant room. Behne [88] evaluated the two systems with chilled ceilings. Cermak et al., [89] analyzed air quality and thermal comfort with the two systems in an office room. In a related study, Cremak and Melikov [90] probed the performance of personalized ventilation in conjunction with the two system types. Yin et al., [91] assessed the performance of the two ventilation systems in relation to the location of the exhaust in a full-scale experimental chamber. Smedje et al., [92] examined the two systems in the light of air quality, airborne cat allergen, and climate factors in the occupied zone in four classrooms of a school building. Hu et al., [93] carried out a comparison of energy consumption between displacement and mixing ventilation systems for different buildings and climates. Lin et al., [94,95] used CFD simulations to compare displacement and mixing ventilation in terms of thermal comfort and indoor air quality. These studies demonstrate that displacement ventilation systems normally have higher values of contaminant removal effectiveness and air change efficiency than mixing ventilation systems.

3. A Novel Application of Displacement Ventilation in Cold Climates

In Norway and other Scandinavian countries, the heating, ventilation, and air conditioning (HVAC) system for school and office buildings is typically a hybrid air-water system. It is customary to use balanced mechanical ventilation with heat recovery to provide overall air quality, along with high energy efficiency in winter and thermal comfort in summer. In recent years, it has also become common to use mechanical cooling or free cooling from ground heat exchangers distributed centrally through the air system [96]. Heating is generally provided through a hydronic system, with radiators and underfloor heating being the most used terminal types. However, ventilation air is usually heated centrally to a supply setpoint, generally a few degrees below the room temperature (typically 17–20 °C).

Until recently, heating buildings and individual rooms with an all-air system have been uncommon in Norway, except for storage facilities and certain industrial buildings with lower demands on thermal comfort. In recent years, however, the widespread introduction of low energy buildings and passive houses [97,98] have created new opportunities for innovative heating solutions. For such buildings with low heating demands, using an all-air system for heating provides a simple and energy-efficient alternative to the conventional hydronic heating systems [97,99]. Demand-controlled ventilation systems that vary airflow with changing heat load in the occupied zone have been used in some passive houses or similar energy standard office buildings [100], and have also been examined in laboratory

tests. These systems have been based primarily on the mixing ventilation principle, giving a rather uniform temperature and air quality in the occupied space.

The concept of providing heating and cooling through an air system has been taken a step further in a newly built Montessori school in Drøbak, Norway. The lower secondary school for 60 students has been built with a heated area of approximately 900 m^2. The school has two levels, with the lower floor underparts of the building where the terrain has a natural fall. The building has a compact rectangular shape oriented southeast-northeast and is intersected by an inclined "solar slice". A photograph of the front of the building is shown in Figure 2. The school has been built with a vision to become Norway's most environmentally friendly school. It is the first school building to fulfil the requirements of the Norwegian Powerhouse-concept [101]. The basis for the design is a well-insulated building envelope with minimized heat loss, a very efficient lighting system, a high-performance ventilation system, and a ground-source heat pump system that provides free cooling in summer. These measures reduce the demand for delivered energy radically, and a building-integrated system with high-efficiency photovoltaic (PV) modules makes the school into a plus energy building according to the Powerhouse-definition. The specifications for the design and simulated energy performance are given in Tables 1 and 2 below.

Figure 2. Drøbak Montessori lower secondary school. (Credit: Robin Hyes, Skanska).

Table 1. Design details of the Powerhouse Drøbak Montessori lower secondary school.

System	Design Parameter	Value
	Floor area (heated)Air volume (heated)	886 m^2 3340 m^3
	U-value external wall	0.14 W/m^2K
	U-value roof	0.09 W/m^2K
	U-value slab on ground	0.10 W/m^2K
	U-value window (average value)	0.75 W/m^2K
	Infiltration at 50 Pa	0.50 ach
	Normalized heat capacity (medium-heavy building)	81 Wh/m^2K
	Average airflowHeat recovery efficiencySpecific fan power	4.0–8.0 m^3/hm^2 86% 0.60 $kW/m^3/s$
	Cooling capacity, cooling coilFree cooling from geothermal wells	17 W/m^2 15 kW
	Heating capacity, heating coilHeating from geothermal heat pump	20 W/m^2 15 kW
	Lighting average load	3 W/m^2
	PV-system module areaEfficiencyPeak load	145 m^2 21% 30 kW

Table 2. Simulated net energy demand and delivered energy for the school.

System	Net Energy Demand (kWh/m^2/year)	Coefficient of Performance (COP)	Delivered Energy (kWh/m^2/year)
Space heating (by air)	18.7	4.5	4.2
Domestic hot water	3.2	3.0	1.1
Fans	3.7	-	3.7
Pumps	1.0	-	1.0
Lighting	6.6	-	6.6
Plug loads	13.0	-	13.0
Ventilation cooling	1.8	15.0	0.1
Total	*48.1*	-	*29.6*
PV Production	-	-	*−37.0*
Net Delivered Energy	-	-	*−7.4*

The HVAC system of the Drøbak Montessori has been designed to achieve the high performance needed to be a plus energy building, but with as simple and robust technology as possible. Heating and cooling to the school are provided by a central air system. The air distribution is based on displacement ventilation that varies between fully mechanical and hybrid ventilation depending on the time of the year. The supply air is provided to classrooms and other spaces via rectangular perforated displacement diffusers installed in the interior walls at low levels. The extract air is removed from the occupied zones at high levels by overflow to the adjacent areas. During summer, the exhaust air is directly discharged to the outside through an opening in the top of the atrium in the center of the building. During winters, the air is mechanically exhausted through the air handling unit after heat recovery.

The HVAC system of the Drøbak Montessori is unique in the aspect that it is based on the displacement ventilation principle and provides heating only outside the occupied periods. During the occupied hours between 7:30 to 16:00 h, the system operates in the "normal mode", in which a VAV (variable air volume) damper regulates flow to each zone to maintain the desired indoor CO_2 (carbon dioxide) concentration and space temperature set-points. The supply air temperature during the normal mode is outdoor temperature-compensated as shown in Figure 3. In the warmest periods, the supply air is provided at 18.5 °C, whereas, in the coldest periods, the supply air temperature is approximately isothermal with the zone air temperature (i.e., 21–22 °C). During occupied hours, the system essentially operates as a conventional displacement ventilation system, by which the air is supplied to the conditioned space at a lower or at most equal temperature to the average air temperature in the zone.

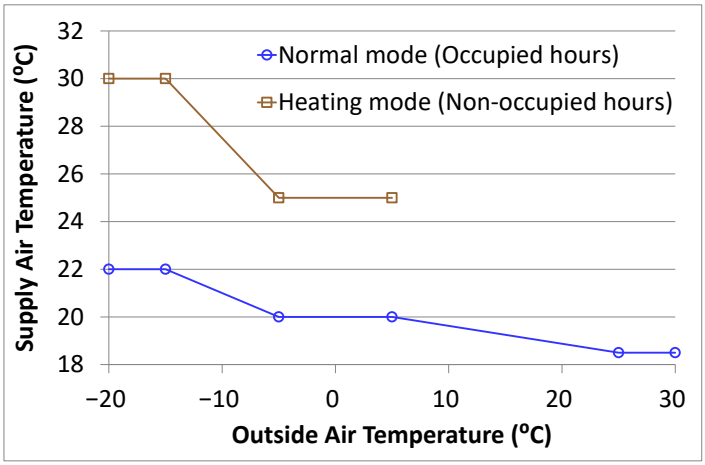

Figure 3. Supply air temperature as a function of outdoor air temperature.

In hot periods in summer the system operates in "night cooling mode" outside occupied hours. The night-time cooling starts when the inside air temperature is above 23 °C and stops when it reaches 20.5 °C. During the night cooling mode, only outside air is used for cooling the space. In Norway and several other European countries, the outdoor air at night, even in summer times, is frequently cooler than the indoor air and can thus provide free cooling. In the night cooling mode, the system operates as a normal displacement ventilation system as the temperature of the supply air is lower than the average air temperature in the zone. However, as there are no heat sources to drive the displacement process, the temperature stratification is less pronounced and there is almost an isothermal condition in the space.

The "heating mode" outside occupied hours turns on when the outside air temperature is below 10 °C, and the room temperature in the three coldest rooms is below 20.5 °C. The heating stops when the temperature is above 22.5 °C in all rooms. In the heating mode, the ventilation system runs in recirculation with no fresh air intake to save energy for heating. In both heating and night cooling modes, the airflow to a zone is set to its maximum design value. In the heating mode, the temperature of the supply air is outdoor temperature-compensated as shown in Figure 3. In the coldest periods, the supply air is provided at 30 °C but the supply air temperature decreases down to 25 °C with increasing outside air temperature. Due to the elevated supply temperatures in heating mode, the vertical stratification in the zone ought not to be the typical distribution of displacement ventilation. The warm air supplied at low levels could rapidly move to the upper level of the space, resulting in a temperature stratification in the space. On the other hand, descending air flows along cold surfaces like windows and, to some degree, external walls would counteract the stratification in the space. Depending on the balance between the plume effect of the elevated supply temperature and the descending air flows from the cold surfaces, the hypothesis is that the temperature profile in the space will be somewhat intermediate between that of full mixing and displacement air distributions.

Still, several issues related to the application and modeling of displacement ventilation for heating during non-occupied hours remain to be fully understood. Some of the most significant and still unresolved questions include: (1) Is heating during the non-occupied hours only enough and will it provide the desired thermal comfort level during the occupied hours? (2) Will the temperature gradient in classrooms be too high at the start of the school day and during the non-occupied hours? (3) Will the warm air supplied with low impulse just ascend to the ceiling, and not heat the lower and occupied space? (4) Is there a risk that with low occupancy in a zone, the internal loads may not be enough to ensure satisfactory thermal comfort conditions in the zone? And (5) is there a risk that with high occupancy in a zone after night mode preheating, the internal loads may be too high to ensure satisfactory thermal comfort conditions in the zone?

4. Method

This paper explores the above-mentioned questions using a combination of experimental tests and numerical simulations. Full details of the experimental and simulation methods used in this study, for analyzing the aptness of displacement ventilation for providing heating during non-occupied periods without a separate heating system, is provided in the following sections.

4.1. Experimental Tests

The experimental methods utilized in this study comprised of laboratory and field tests. The lab tests were performed on a scaled classroom model under carefully controlled laboratory conditions. The field test was carried out in an actual classroom under real uncontrolled field conditions. The methodology of the experimental tests is described below in detail.

4.1.1. Lab Tests

The validity of the design concept has been verified through lab testing of a simplified unscaled model of the classroom. The laboratory testing was carried out at the Building and Infrastructure test facility of SINTEF in Oslo. The test room was built inside a lab hall with controlled indoor conditions of 18 °C. The mock-up classroom had a floor area of 4.0 m × 4.0 m and a height of 3.0 m. The room walls and ceiling were made of 100 mm polyurethane foam/aluminum sandwich elements. The floor consisted of two 40 mm precast concrete slabs bonded together with and overlaid with a bituminous mix, 10 mm EPS insulation, and 0.15 mm of building plastic. The joints between the construction elements were filled with foundry sand and then spackled. The U-value for walls and ceiling was 0.2854 W/m^{2}K and for the floor was 0.2816 W/m^{2}K.

Figures 4 and 5 show the floor plan and photos of the test room with installed equipment, measurement setup, and heat sources. A displacement ventilation system was installed for providing heating and ventilation to the mockup classroom. The supply air to the classroom was provided through a semi-circular displacement diffuser mounted on the south wall connected with a 125 mm circular supply duct. The part of the air duct located in the room was insulated with 4 mm cellular plastic. The supply airflow was controlled by means of a modulating damper, which, in turn, was regulated by a high-accuracy airflow sensor. Air was exhausted passively via a 125 mm circular ventilation duct located at the opposite end of the room, 0.2 m from the ceiling and the north wall.

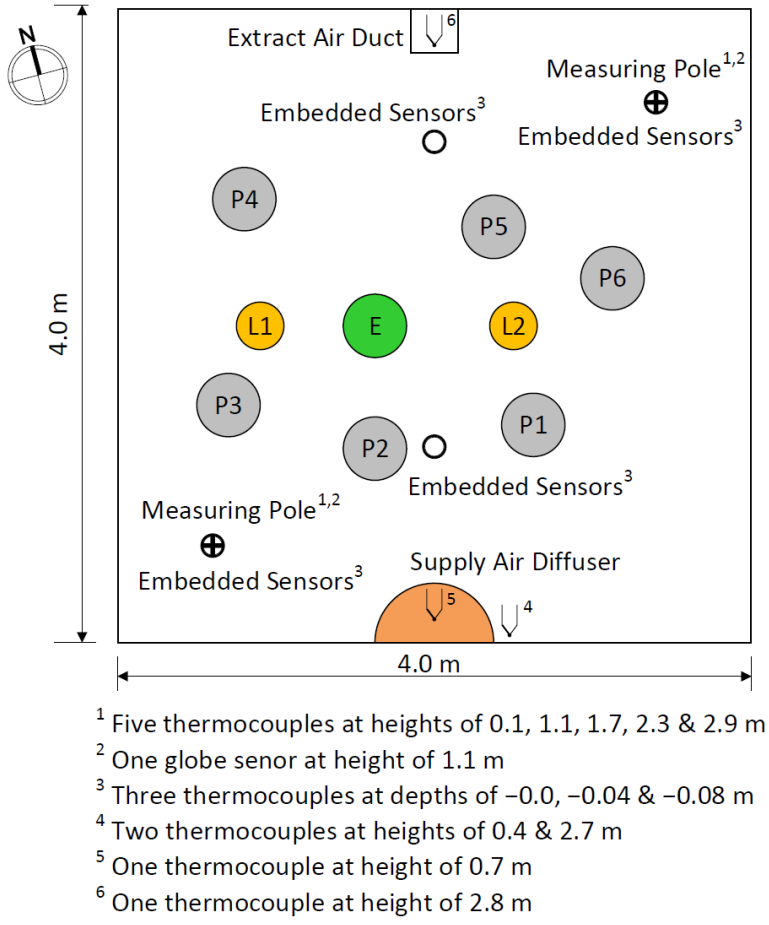

[1] Five thermocouples at heights of 0.1, 1.1, 1.7, 2.3 & 2.9 m
[2] One globe senor at height of 1.1 m
[3] Three thermocouples at depths of −0.0, −0.04 & −0.08 m
[4] Two thermocouples at heights of 0.4 & 2.7 m
[5] One thermocouple at height of 0.7 m
[6] One thermocouple at height of 2.8 m

Figure 4. Floor plan of the test room with measurement points and internal heat sources (people: grey, lighting: yellow, equipment: green).

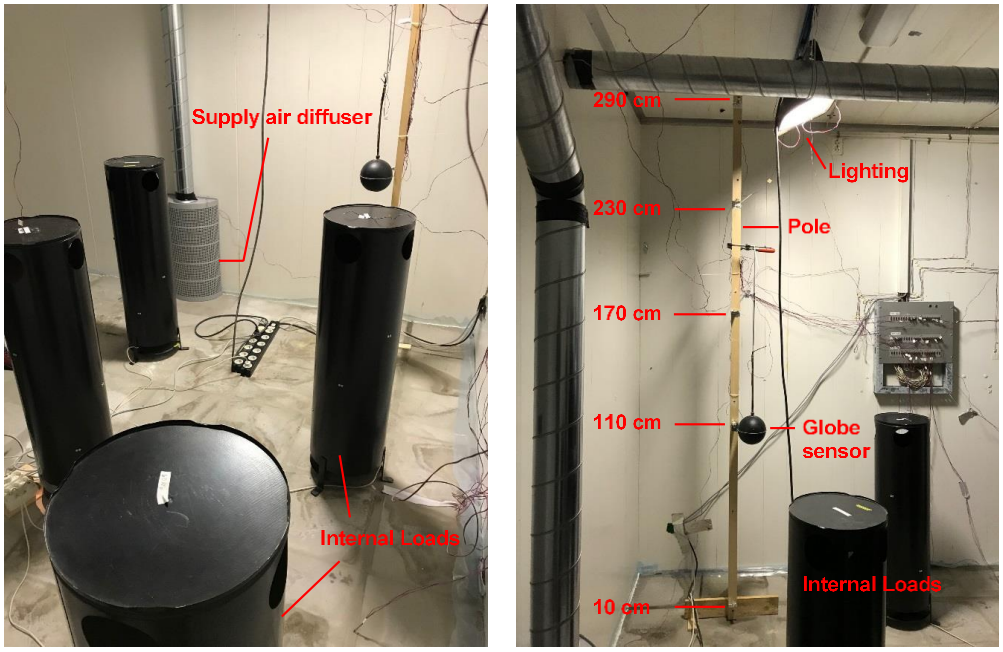

Figure 5. Photos of the test room with measurement points and internal heat sources.

In the test room, internal heat gains from people, equipment and lighting, and transmission losses through the outer walls were simulated experimentally for two distinct scenarios with different occupancy patterns, and thus with different airflows, internal loads, and transmission losses. The first scenario, Scenario I, corresponded to a typical situation in which the classroom is fully occupied throughout the day, from 8:00 until 16:00 h, except during the lunch break, between 11:00 and 12:00 h, when the classroom is empty. The second scenario, Scenario II, corresponded to a specific situation when the classroom is occupied only during the afternoon between 13:00 and 16:00 h with 50% of the design occupancy level. Both scenarios were simulated experimentally for 48 h. During the experimental testing, thermal manikins with a nominal power of 40–120 W and a convective heat fraction of approximately 0.5 were used for simulating heat loads from people and equipment. Heat loads from lighting were provided through incandescent bulbs with a nominal power of 2 × 40 W. Figure 6 presents the daily internal loads from people, equipment and lighting, and supply air temperatures and flows simulated for the two scenarios. Transmission losses through the outer walls were simulated by circulating cold water in pipes integrated into the east and west side walls of the test room. The supply temperature and mass flow of the circulating water were chosen to emulate the transmission losses through the external walls during the occupied hours at an outside temperature of −15 °C.

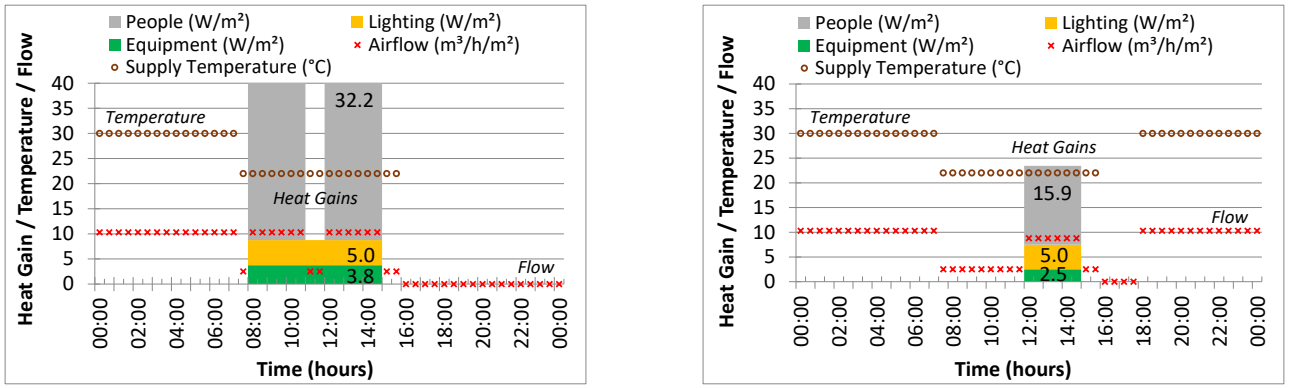

Figure 6. Specific internal heat gains, specific airflows, and supply air temperatures for Scenario I (**left**) and Scenario II (**right**).

The measurement setup used in the test room was shown above in Figures 4 and 5. The supply and exhaust air temperatures were measured in the supply air diffuser and the return air duct, respectively. The temperature profile of the room air was measured at two different positions in the SW and NE parts of the room. Two vertical poles, each with five measurement points at heights of 0.1, 1.1, 1.7, 2.3, and 2.9 m above the floor level, were used for measuring air temperature stratification in the room. Temperature distribution in the floor slab was measured at depths of 0, 4, and 8 cm below the floor level at four different positions in the room, with two positions being directly below the vertical poles. All the temperature measurements were made with calibrated thermocouples of type T, class 1, which had an accuracy of ±0.5 K in the measured temperature range. Each vertical pole also had an additional globe temperature sensor, with a measurement accuracy of ±0.1 K, installed at the sitting height to measure the radiant heat temperature in the room. The airflow measurements were taken in the supply air duct using a differential-pressure-based flow measurement station with a measurement tolerance of less than 4%. The transmission losses from the external walls were measured using calibrated heat meters.

4.1.2. Field Test

An in-situ field test was carried out in a pentagon-shaped classroom on the lower level of the Drøbak Montessori school building. Figures 7 and 8 show the floor plan and photos of the classroom with the measurement setup. The classroom had a floor area of 52.2 m^2 and a ceiling height of 3 m. It had a medium-weight construction, with a well-insulated thermal envelope and a high window-to-wall ratio. The classroom had two exterior walls located on the southwest and southeast sides and three interior walls located on the north, east, and northwest sides. The total area of the interior and exterior walls was 44.7 m^2, and 42.9 m^2, respectively. The heat transfer coefficient (U-value) and heat capacity of interior walls were 0.26 W/m^2K and 2.4 Wh/m^2K, respectively. The exterior walls had a heat transfer coefficient and an inner heat capacity of 0.14 W/m^2K and 2.4 Wh/m^2K, respectively. Floor and ceiling had heat transfer coefficients of 0.10 and 0.25 W/m^2K, respectively, and heat capacities of 63, and 3.0 Wh/m^2K, respectively. Windows (glazing and frames, combined) covered 43.8% of the total exterior wall area and had a heat transfer coefficient of 0.75 W/m^2K.

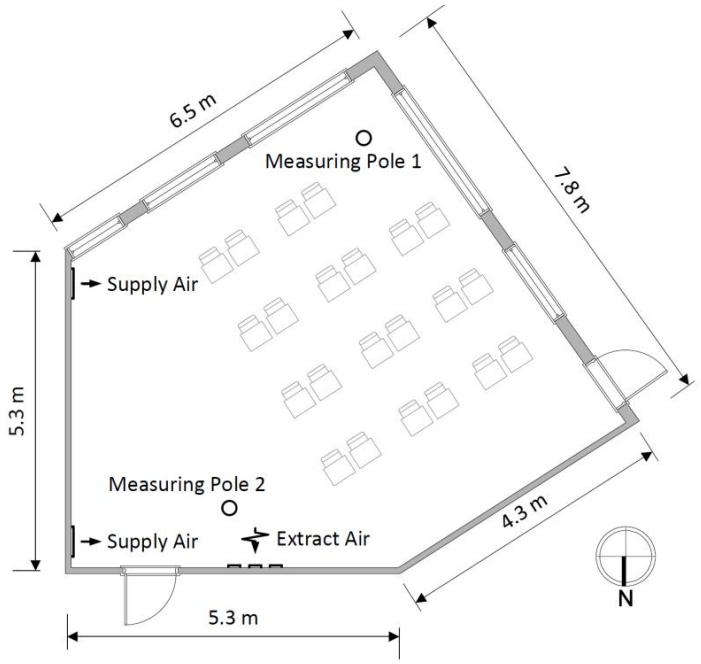

Figure 7. Floor plan of the classroom with measurement points.

Figure 8. Photos of the classroom with measurement points for temperature and CO_2.

The classroom was supplied with air from a central air handling unit. The airflow in the classroom was driven by displacement ventilation. The supply air to the classroom was provided through two wall-embedded supply air diffusers installed 50 mm above the floor level at the far ends of the east-facing inner wall. The 600 mm × 900 mm rectangular air diffusers were connected to a 315 mm circular main supply duct via two feeder ducts. The airflow in the main duct was regulated by a modulating damper, which was controlled in response to air temperature and CO_2 concentration in the classroom as described previously in Section 3. The maximum allowable design airflow from each supply diffuser was limited to 264 m^3/h to not exceed a sound power level of 25 dB(A). At maximum airflow, each diffuser had a near-zone distance of less than 1.5 m to the 0.20 m/s isovel, measured 0.1 m above the floor level with a 3 K temperature difference between the room and supply air temperatures. Air from the classroom was extracted via three extract air grills installed 2.8 m above the floor level in the top center of the north-facing inner wall. Passive overflow elements with sound attenuators were used to transfer the extract air to the corridor outside the classroom, from where it was collected and returned to the air handling unit.

Figure 9 presents the internal loads from people, equipment, and lighting, solar gains through the room fabric, and supply air temperatures and flows for the field test. The field test was performed for approximately 16 h on a cold winter day with ambient air temperatures ranging between −7 and +3 °C. From the start of the test at midnight, up until 7:30 a.m., the displacement ventilation system operated in the heating mode, supplying recirculation air to the classroom at a rate of approximately 10.5 $m^3/h/m^2$ floor area and at outdoor temperature-compensated supply temperatures between 27.1 and 28.1 °C. At 7:30 a.m., the displacement ventilation system switched from the heating mode to the normal mode. In this mode, the supply air temperature and flow to the room were originally designed to be regulated by outdoor temperature, and the indoor temperature and CO_2 levels, respectively. However, for the field test, the supply air temperature and flow to the classroom were purposefully chosen to represent a nearly impossible worst-case scenario. The supply air to the classroom was provided at temperatures between 16 and 18 °C, which were 3 to 4 °C below the actual design values. The supply airflow to the classroom was set constant and approximately equal to the maximum design flow. The classroom was occupied between 08:00 a.m. and 03:30 p.m. The internal loads in the classroom varied throughout the day, as it normally happens in classroom contexts. Between 08:30 a.m. and 02:30 p.m., thirteen to nineteen persons were present in the classroom at any one time,

except the lunch break from 11:30 a.m. to 12:30 p.m. when the classroom was completely unoccupied. Internal loads from equipment and lighting were fairly constant throughout the day. Solar heat gains transmitted through the room fabric, including windows and walls deduced from the measured solar irradiance data from a nearby weather station using TEKNOsim 6 software [102] were as high as 450 W (i.e., 8.6 W/m^2 floor area). Heat losses through classroom envelope and ventilation and infiltration were simulated and are presented in Section 5.2.2.

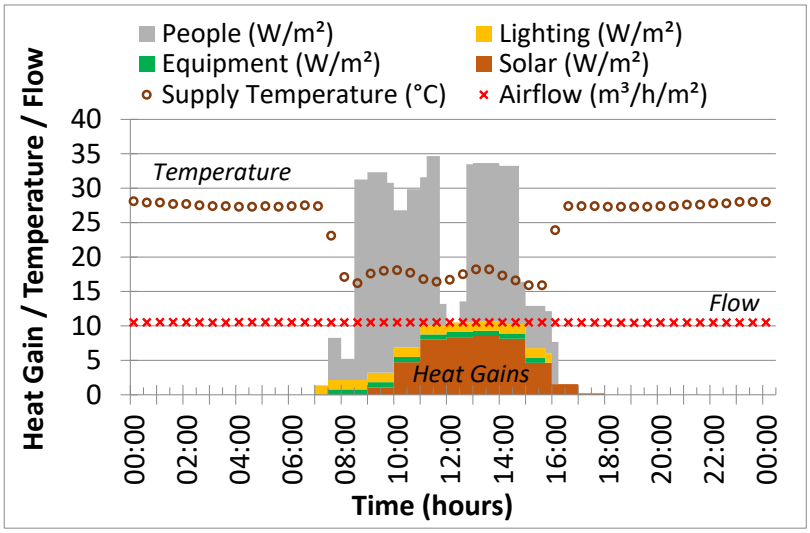

Figure 9. Specific internal heat gains, specific airflows, and supply air temperatures for the field test.

The measurement setup in the classroom consisted of sensors for measuring air temperature, radiant temperature, CO_2 concentration, and airflow and airspeed. The temperatures of supply and extract air to and from the room were measured by sensors installed in supply air diffusers and return air grilles. Two instrumented vertical poles, placed in the south and east corners of the classroom, were used for measuring air temperature and CO_2 stratification in the room. Each pole had a set of temperature and CO_2 sensors installed at four different heights of 0.1, 1.1, 1.7, and 2.7 m. All air temperature sensors had an operating range of −20 to 70 °C, an accuracy of ±0.21 °C, and a resolution of 0.024 °C. The CO_2 sensors had an accuracy of ±50 ppm over the measured concentration range. Each vertical pole also had an additional globe temperature sensor and an omnidirectional anemometer installed at approximately the standing height for measuring the radiant heat temperature and air velocity, respectively. The measurement accuracies of the globe sensor and anemometer were ±0.1 K, and ±0.04 m/s, respectively. The supply airflow to the room during the occupied period was measured using a thermal anemometer with a measurement tolerance of less than ±4%. The airflow outside the operating hours was obtained from the centrally measured BMS data.

4.2. Simulation Studies

Simulations of experimental studies of the previous sections were performed to assess the suitability of a commonly used transient dynamic method for predicting the thermal and contaminant stratification in the displacement ventilation systems. The simulations were performed using IDA-ICE, which is a commercially available state-of-the-art building performance simulation for performing a multi-zonal and dynamic study of indoor climate, energy, and daylighting. The software is reported to be validated in accordance with several European and International standards, including Standard EN 15265 [103] and ASHRAE Standard 140 [104], among others. The Climate model in IDA-ICE version 4.8 SP1 was used for performing the transient simulations of temperature stratification and CO_2 concentrations. The Climate model uses multi-node calculations to determine temperatures

of different surfaces in the zone and different layers in the construction. The indoor environmental conditions in both horizontal and vertical directions are determined using a detailed physical model of the building and its components. A significant limitation of the Climate model is that it cannot be used for simulating irregular and asymmetrical zone geometries. The zone geometry must be simplified to a rectangular footprint before the simulations can be performed.

In the climate model, air distribution to a zone is classified as mixing or displacement ventilation. For displacement ventilation, air temperature at the floor level is determined by using an energy balance between the convective heat transfer from the floor surface to the air at the floor level and the ventilation heat flux from the supply air. The air temperature at the ceiling level is computed by considering the heat capacity of the zone air volume and accounting for all heat transfer to the zone air. Based on the calculated air temperatures at floor and ceiling levels, a linear temperature gradient is calculated for the zone using the Mundt model [28]. Temperatures at the zone surfaces are also interpolated between the floor- and ceiling-level air temperatures. Alternatively, a fixed linear temperature gradient can be specified directly by the user. In that case, the air temperature at the floor level is obtained using the air temperature at the ceiling level and the provided gradient. If the thermal gradient disappears or becomes negative, the air distribution is treated as mixing ventilation instead.

The CO_2 concentration in the Climate model is determined based on the balance between the CO_2 generated in the zone and the CO_2 concentration in the ventilation air supplied to the zone. The CO_2 generated from occupants is modeled as a function of their activity level. A significant limitation of the model is that the CO_2 concentration for each time step is calculated as a single average value over the zone volume. Therefore, the model does not account for the vertical stratification of the CO_2 concentration in the zone. Moreover, it also does not consider the change in CO_2 concentration with distance from the emission source.

4.2.1. Lab Test

A simulation model of the mock-up classroom used for the lab tests was built in IDA-ICE. The simulation model was constructed using the actual geometry and construction parameters of the test room described in detail in Section 4.1.1. A constant temperature boundary condition of 18 °C was imposed on all envelope elements except the external walls to match the onsite test conditions. The transmission heat losses through the outer walls were modeled using a controller macro, which split the total losses equally over the two external walls. Inputs to the simulation model included internal loads, operating schedules, and supply air temperatures and flows. These inputs were acquired from the site-controlled and measured test conditions shown in Figure 6. The test data was however processed to 15-min time steps used for the simulation. The Climate model in IDA-ICE was used to simulate the vertical temperature gradients. Cyclic runs of each simulation scenario were performed before the result-generating simulation run to ensure stable conditions. As there were no emission sources in the zone, the CO_2 concentrations in the mock-up classroom were not simulated.

4.2.2. Field Test

The simulation model of the whole school building including the classroom used in the field test was built in IDA-ICE. For the simulation model, the geometry of the actual classroom used in the field test was simplified to a rectangular footprint. This was because the climate model in IDA-ICE could not simulate irregular and asymmetrical zone geometries. Nevertheless, the model was customized to match the volume, floor area, and climate envelope area of the actual classroom. Figure 10 shows the geometries of both the actual room and the simplified simulation model built in IDA-ICE. The actual classroom was shaded from terrain and trees surrounding it. The shading effect was estimated based on onsite observations and was incorporated in the simulation model through vertical

shading elements with 0% transparency for terrain-elements and 50% transparency for tree-elements. Figure 11 shows the building model with modified classroom geometry and the surrounding vertical shading elements as implemented in IDA-ICE.

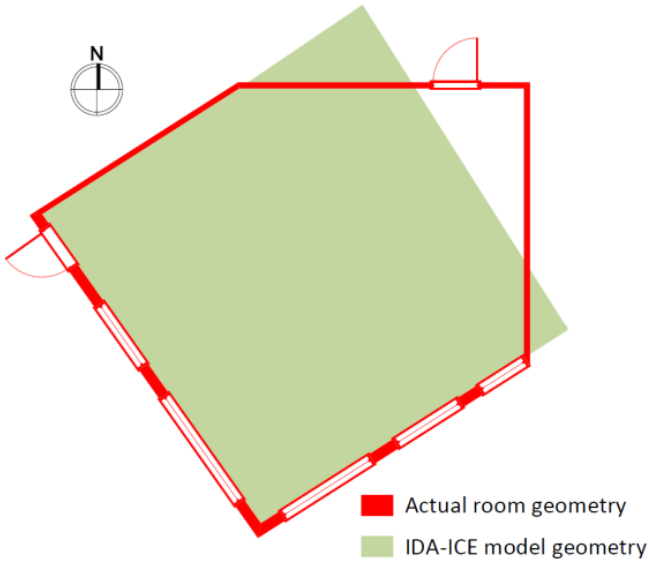

Figure 10. Actual and modeled geometries of the classroom.

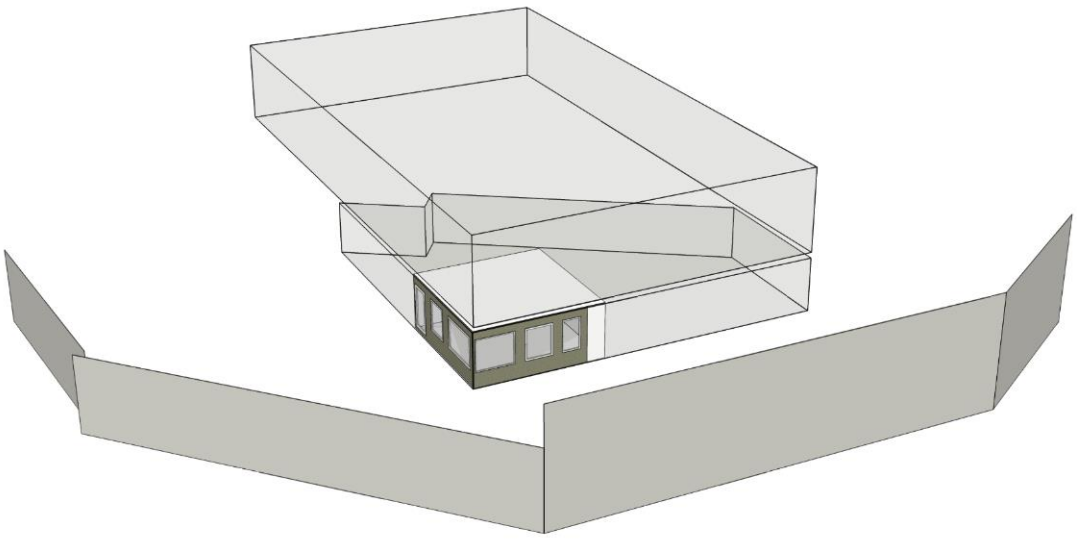

Figure 11. Implemented building model in IDA-ICE.

As for the lab model, the actual construction details of the classroom, presented earlier in Section 4.1.2, were used to build the simulation model. The inputs to the simulation model included the specific schedule used for the test, the dynamic internal loads, and the actual supply air temperatures and flows. The climate file used for the simulation was based on the combination of weather data for the actual area in the simulated period and standardized values for a typical year for Oslo. The outdoor temperature and solar data were based on actual measurements. The outdoor temperature data was measured on-site whereas the solar data was taken from a nearby weather station. The solar data was processed using TEKNOsim algorithms [102] to determine direct and diffused components to be used in the climate file of IDA-ICE. Temperatures in adjacent rooms and spaces were also

based on measured values. The ground reflection (albedo) was set to 0.6 based on observed values on the test day. The calculated solar heat gains were as high as 450 W (i.e., 8.6 W/m^2 floor area). The model simulated transmission losses through the classroom envelope based on the room envelope areas, heat transfer coefficients, and the temperature difference on each side of the envelope. One issue in simulating the transmission heat losses was to model the ground heat losses accurately. This was because the field test was performed just after the completion of the building, which did not allow construction enough time to dry out and stabilize before the field test. To overcome this issue, the external floor was modeled considering a constant ground temperature of 0 °C. Furthermore, the thermal conductivity of the insulation in the external floor construction was adjusted to account for the moisture in the slab. The model also simulated heat losses due to ventilation and infiltration. The ventilation heat losses were modeled using the measured ventilation rates, whereas the infiltration heat losses were modeled based on the calculated air leakage to the outside and surrounding zones.

The vertical temperature gradients were simulated using the Climate model in IDA-ICE. The simulations were performed using a dynamic startup and cyclic runs were made to ensure stable conditions before the result-generating simulation. The measurement points in the simulation run corresponded to actual sensor locations used in the field test. The CO_2 concentrations in the zone over time were also simulated using the Climate model. An activity level value of 1 MET, corresponding to sitting quietly, and an atmospheric CO_2 concentration of 400 ppm was used for the simulations.

5. Results

In this section, the results of experimental tests and numerical simulations described above are critically presented and discussed, giving a detailed insight into the performance of the displacement ventilation for providing heating during non-occupied periods without the need for a separate heating system.

5.1. Experimental Results

The results of two lab tests carried out in the scaled mock-up classroom under carefully controlled laboratory conditions and one field test performed in the full-scale classroom under actual field conditions are presented in the following sections.

5.1.1. Lab Test

Figure 12, left and right, show measured values of supply, extract and operative temperatures, and airflows for Scenario 1 and Scenario 2 of the lab test. The only noticeable difference between the measured values of Figure 12 and the originally planned values of Figure 6 is in the supply air temperature in the heating mode at night. For both scenarios, the actual supply air temperature in the heating mode was around 29 °C, which was 1 K lower than the originally planned value. This discrepancy was caused because the supply air temperature to the test room was regulated by a sensor located in the air duct, 2.8 m above the supply air diffuser, whereas the measurements of supply air temperature shown in Figure 12 were taken with a sensor placed in the supply air diffuser at 0.7 m height. Hence, in the heating mode, there was a duct heat loss of 1 K to the room due to the large difference in the temperature of the air in the duct and the temperature of the air in the room. In the normal mode, the supply air temperature in both scenarios was approximately 22 °C as originally planned. For both scenarios, the room operative temperature was between 22–24 °C when occupied. The extract air temperature from the room depended upon the operation mode of the system and the occupancy level. For both scenarios, the extract air temperature in the heating mode was 5–7 K lower than the supply air temperature. For Scenario 1, which corresponded to a situation in which the classroom was fully occupied between 8:00–11:00 and 12:00–16:00 h, the extract air temperature in the normal mode was on average 1.7 K and maximum 2.2 K higher than the supply air temperature. For Scenario 2, which corresponded to a situation in which the

classroom was occupied only during the afternoon between 13:00 and 16:00 h with 50% of the design occupancy level, the extract air temperature in the normal operating-mode was only occasionally and marginally higher (<0.5 K) than the supply air temperature.

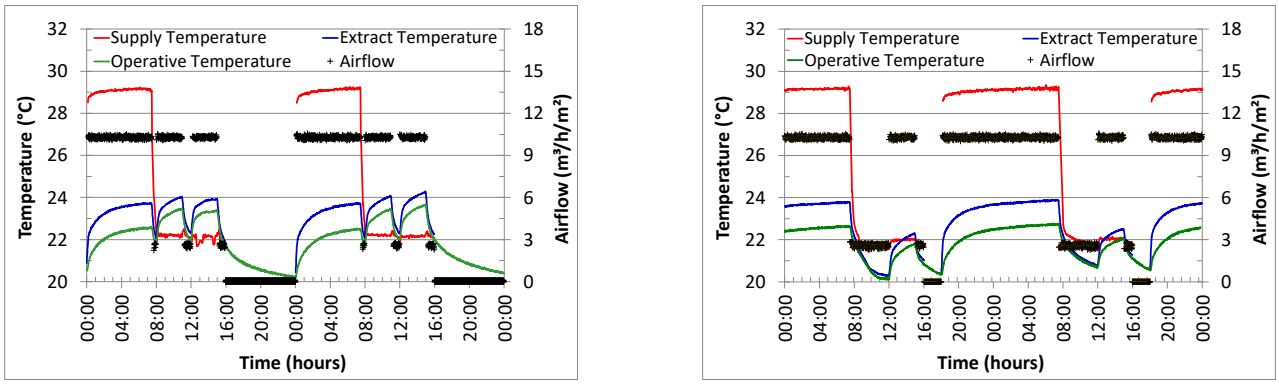

Figure 12. Measured supply, extract, and operative temperatures, and airflows for Scenario I (**left**) and Scenario II (**right**) of the lab test.

Figure 13 shows the vertical temperature profiles at heights of 0.1, 1.1, 1.7, 2.3, and 2.9 m above the floor level for the two scenarios. Each curve represents an average of two temperature sensors installed at the same height on the two instrumented poles in the opposite corners of the test room. For Scenario 1, the average and maximum vertical temperature gradient between the standing head height (1.7 m) and ankle height (0.1 m) was 1.2 K and 1.4 K, respectively, during the heating mode between 00:00–8:00, and 0.8 K and 1.2 K, respectively, during the normal mode between 8:00–11:00 and 12:00–16:00. During periods of no ventilation between 16:00–00:00, there was no vertical temperature gradient and consequently no stratification. For Scenario 2, the average and maximum vertical temperature gradient between the standing head height (1.7 m) and ankle height (0.1 m) was 1.2 K and 1.4 K, respectively, during the heating mode between 00:00–7:30, and 0.4 K and 0.6 K, respectively, during the normal mode between 12:00–15:00. During periods of no occupancy between 07:30–12:00 and 15:30–18:00, there was no vertical temperature gradient and consequently no stratification.

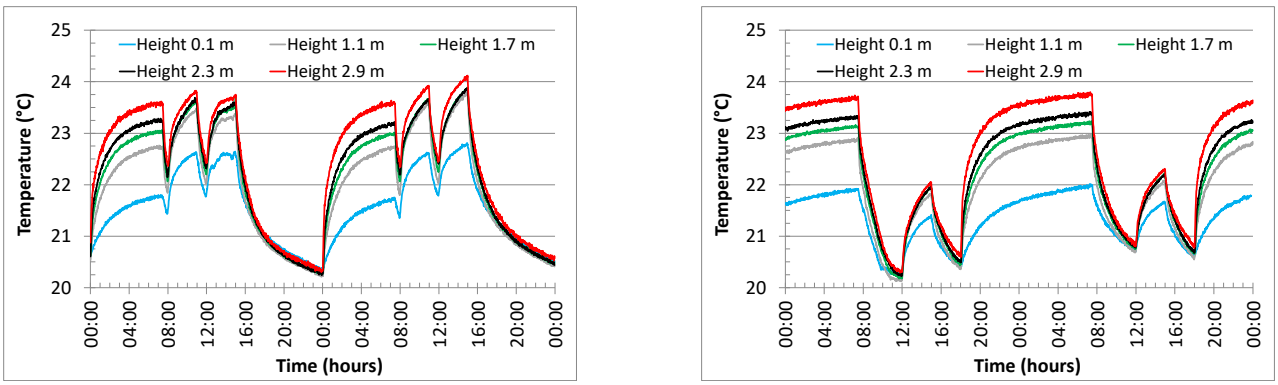

Figure 13. Measured vertical temperature profiles for Scenario I (**left**) and Scenario II (**right**) of the lab test.

Figure 14 presents the vertical temperature distribution in the floor slab at the depths of 0, 4, and 8 cm below the floor level for the two test scenarios. Each curve represents an average of four thermocouples installed at the same depths in different positions in the room. In both scenarios, the slab temperatures increased with time in the heating mode, and its thermal mass was charged. The slab temperatures also increased in the day operating mode, but at different rates, as occupancy levels were dissimilar for the two

scenarios. The discharging occurred in non-occupancy periods when the airflow to the test setup was reduced to zero. Throughout the experiment, temperatures at 8 cm depth remain noticeably higher than the temperatures at 0 and 4 cm depths.

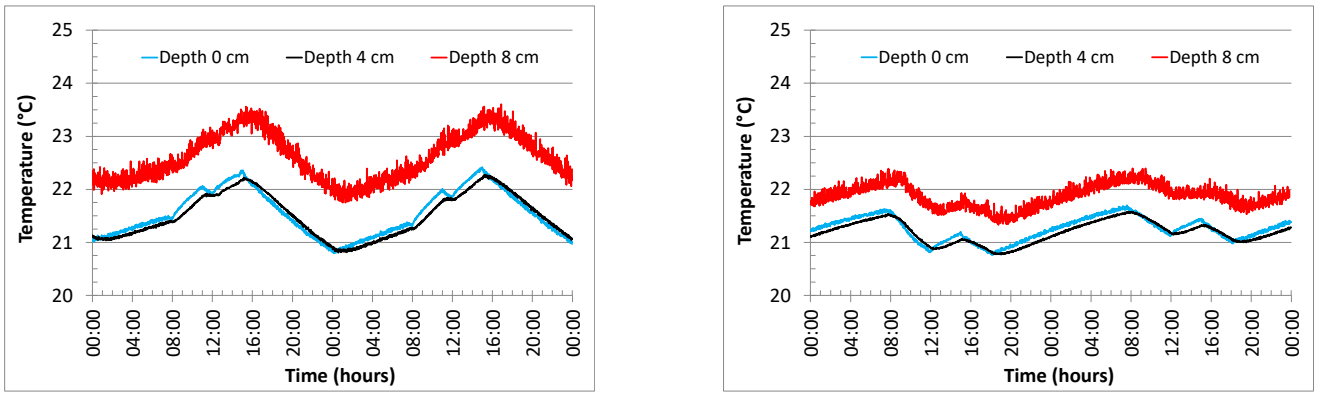

Figure 14. Measured slab temperatures for Scenario I (**left**) and Scenario II (**right**) of the lab test.

5.1.2. Field Test

Figure 15 shows measured values of supply, extract and operative temperatures, and airflows for the field test. Each temperature measurement in the figure is an average of two different sensors. The supply air temperature was measured in each of the two supply air diffusers. Similarly, the extract air temperature was measured in the two extract air grilles. The radiant air temperature was measured by the globe temperature sensor installed on each measurement pole. The operative temperature was calculated based on the measured air temperature, mean radiant temperature, and air velocity according to ISO 7726 [105].

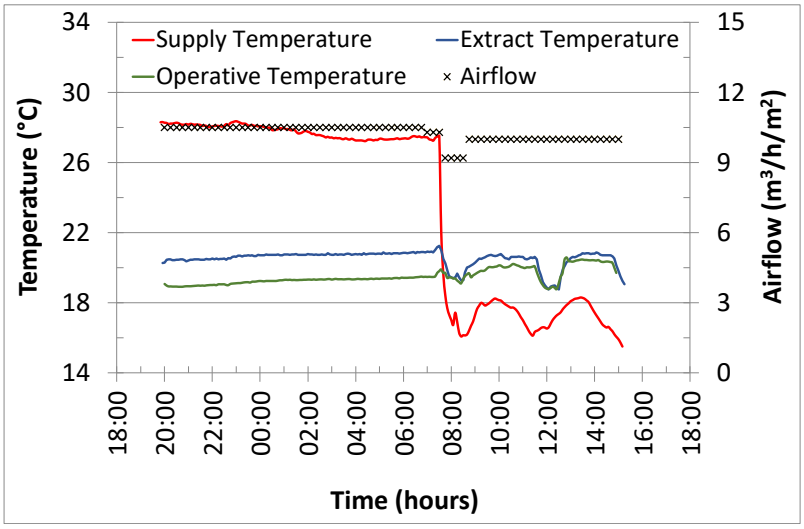

Figure 15. Measured supply, extract, and operative temperatures, and airflows for the field test.

As seen from the figure, the supply air temperature in the heating mode was approximately between 27.3 and 28.3 °C. The supply air temperature in the normal mode varied between 16.1 and 18.3 °C. In both heating and normal modes, the actual supply air temperatures were different from the originally planned outdoor temperature-compensated supply temperatures shown in Figure 3. In the normal mode, the supply temperature was considerably lower than the anticipated value of around 20 °C, primarily due to an anomaly in the supply temperature curve in the control system. This was because the school building was not fully finished at the time of field testing, and the control system

was being tested and commissioned. Nevertheless, supplying air at lower temperatures than originally planned in the normal operation mode provided an even more stringent test of the concept. As in the lab test, the extract air temperature from the room depended upon the operation mode of the system and the occupancy level. In the heating mode, the extract air temperature was 6–8 K lower than the supply air temperature, whereas, in the normal operation mode, the extract air temperature was on average 3.0 K and at maximum 4.4 K higher than the supply air temperature. During the lunch break, the extract air temperature was just under 19 °C due to lower internal heat loads. The operative temperature in the room was rather constant. In the heating mode, the operative temperature was between 19.0 and 19.5 °C. In the normal mode, the operative temperature ranged between 19.3 to 20.5 °C, with an average of 20.2 °C. During the lunch break, the operative temperature was just below 19 °C.

Figure 16 shows the vertical temperature profiles at heights of 0.1, 1.1, 1.7, and 2.7 m above the floor level. Each curve is an average of two sensors mounted at the same height on different poles in the opposite corners of the classroom. As seen from the figure, a vertical temperature gradient was present in the room in both the day operating and the heating modes. The air temperature was lowest at the floor level and rose steadily with height. The average and maximum vertical temperature gradient between the standing head height (1.7 m) and ankle height (0.1 m) in the normal mode was 1.2 K and 1.6 K, respectively, and in the heating mode was 0.5 K, and 0.7 K, respectively.

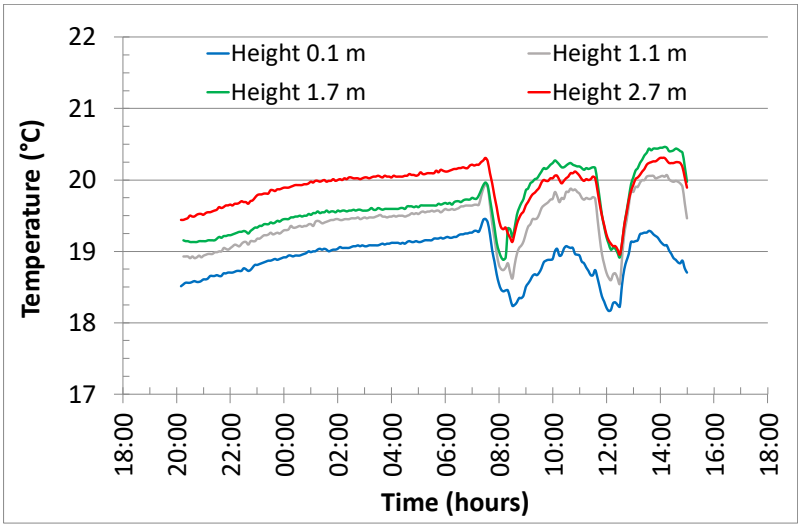

Figure 16. Measured vertical temperature profiles for the field experiment.

Figure 17 presents the vertical CO_2 profiles at heights of 0.1, 1.1, 1.7, and 2.7 m above the floor level. Again, each curve represents an average of two measurements taken at the same heights by sensors mounted on two different poles in two opposite corners of the classroom. The figure shows that in the heating mode there was no vertical stratification of CO_2 in the classroom. This is because there were no CO_2 sources in the classroom. In the heating mode, the CO_2 levels in the classroom decayed to nearly outdoor levels by dilution with the recirculation air. During the normal mode, there was a vertical stratification of CO_2 in the classroom. The CO_2 concentration was lowest at the floor level in the classroom and increased non-linearly with height. Above the sitting head height (1.1 m), the CO_2 concentration had a rather flat gradient. During the lunch break between 11:00 and 12:00 h, and at the end of the school day, the CO_2 concentration in the classroom decayed very rapidly.

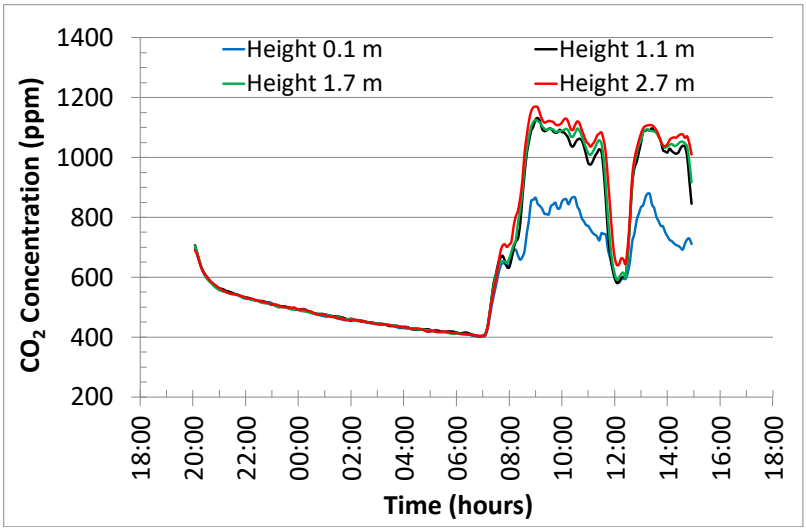

Figure 17. Measured vertical CO_2 concentrations for the field experiment.

5.2. Simulation Results

The results of numerical simulation conducted using IDA-ICE simulation software for the two lab tests and one field test performed, respectively, in the scaled mock-up and the actual classroom are presented in the following sections.

5.2.1. Lab Test

As mentioned earlier in Section 4.2.1, the simulation model of the test room was constructed using the actual geometry and construction details. The inputs to the simulation model including internal loads, operating schedules, and supply air temperatures and flows were based on actual measured data from the lab test. The simulated energy balances of the test room are shown in Figure 18 for the two scenarios of the lab test. As seen from the figure, the heat provided through the displacement ventilation system in the night heating mode was simulated to be partly stored in the room and partly lost through the room envelope. The simulation results implied that in normal mode the stored heat was released back to the room gradually over time, especially during periods of no occupancy and reduced ventilation flows. Moreover, for both Scenario I and Scenario II, the stored heat was simulated not to be released to the room when occupied. This was because the sum of internal heat gains from people, equipment and lighting, and heat gains from ventilation airflow did not exceed heat losses through the room envelope during the occupancy periods.

Figure 19 shows the simulated vertical temperature profiles at heights of 0.1, 1.1, 1.7, 2.3, and 2.9 m above the floor level for the two scenarios of the lab test. For Scenario 1, the model did not simulate any stratification for the heating mode between 00:00–8:00. For periods with normal mode between 8:00–11:00 and 12:00–16:00, the average and maximum vertical temperature gradient between the standing head height (1.7 m) and ankle height (0.1 m) simulated by the model was 0.4, and 0.8 K, respectively. For periods of no ventilation between 16:00–00:00, no stratification was simulated by the model, as expected. For Scenario 2, no stratification was predicted in heating or normal modes. The simulated vertical temperature gradients in both scenarios were lower than the experimentally measured gradients.

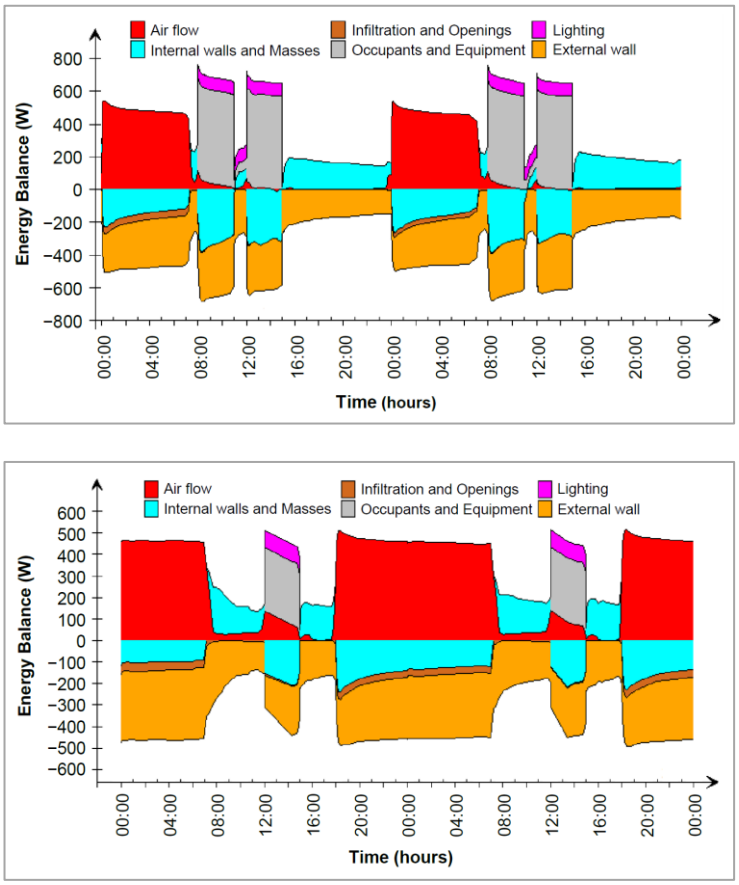

Figure 18. Simulated energy balance for Scenario I (**top**) and Scenario II (**bottom**) of the lab test.

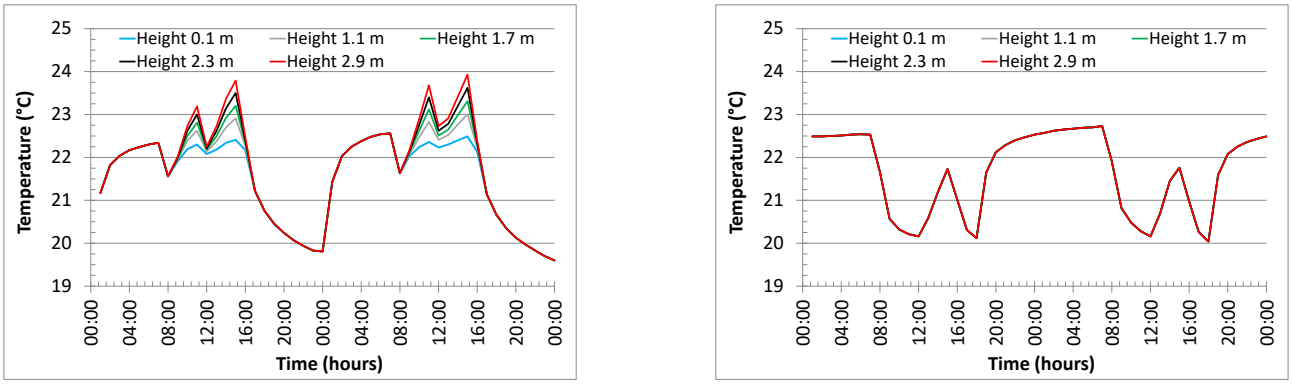

Figure 19. Simulated vertical temperature profiles for Scenario I (**left**) and Scenario II (**right**) of the lab test.

5.2.2. Field Test

Figure 20 shows the simulated energy balance for the field test. As for the lab test, the simulation results of the field test also demonstrated that part of the heat provided through the displacement ventilation and stored in the room structure in the night heating mode was released back to the room during the periods of no occupancy and reduced ventilation in the normal operating mode. Unlike the lab test, heat gains from solar radiation through the windows in the normal mode provided a useful contribution to the energy balance of the classroom. Moreover, ventilation losses in the normal mode had a sizeable contribution to the energy balance of the classroom for the reason that ventilation

air to the classroom was supplied at fairly low temperatures in order to represent a worst-case scenario.

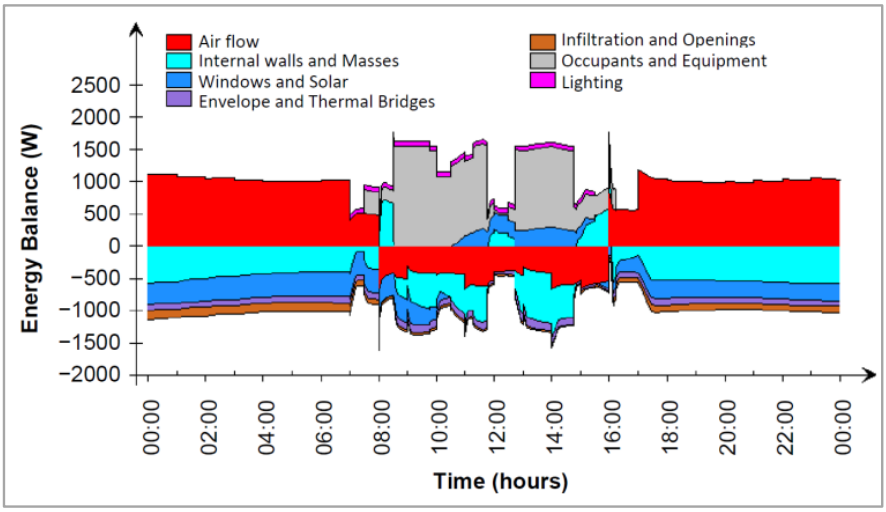

Figure 20. Detailed energy balance for the simulated classroom model.

Figure 21 shows the simulated vertical temperature profiles at heights of 0.1, 1.1, 1.7, and 2.7 m above the floor level. As seen from the figure, the model did not simulate any temperature stratification in the heating mode between 20:00–8:00. In the normal mode, the model simulated a vertical temperature gradient in the room. The air temperature was lowest at the floor level and rose linearly with height. The average and maximum vertical temperature gradient between the standing head height (1.7 m) and ankle height (0.1 m) simulated by the model was 1.5 K, and 1.8 K, respectively. The simulated gradient values were greater than the experimentally measured ones.

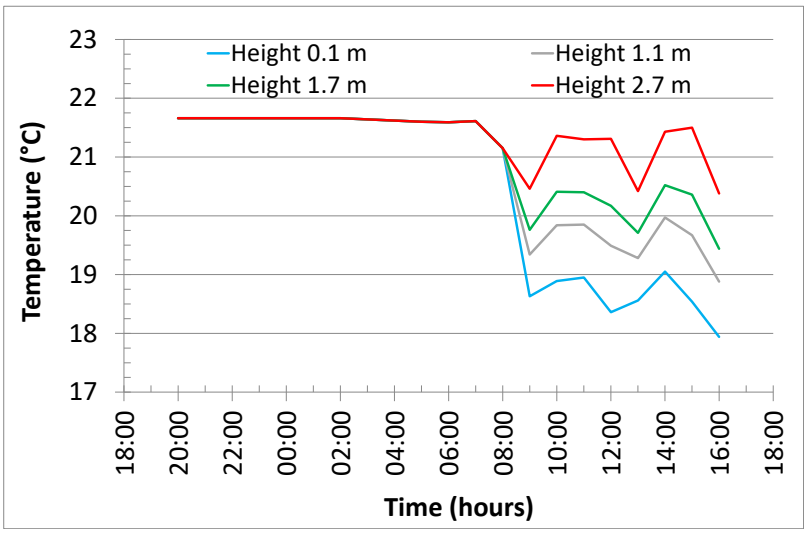

Figure 21. Simulated vertical temperature profiles for the field experiment.

Figure 22 presents the simulated CO_2 concentration in the classroom during the field experiment. As noted earlier in Section 4.2, the IDA-ICE model could only apply a simple CO_2 balance in the zone and could not calculate vertical stratification or horizontal gradient of CO_2 concentration in the zone. The figure shows that in the heating mode between 20:00–8:00 when there were no CO_2 sources present in the classroom, the simulated CO_2 concentration in the classroom was equal to the outdoor concentration. In the normal mode

between 8:00–11:00 and 12:00–16:00, the model only predicted an average value of CO_2 concentration at each time based upon the number of occupants in the classroom and their assigned activity levels. During the lunch break between 11:00 and 12:00 h and at the end of the school day, the model predicted a near exponential decay in CO_2 concentration in the classroom.

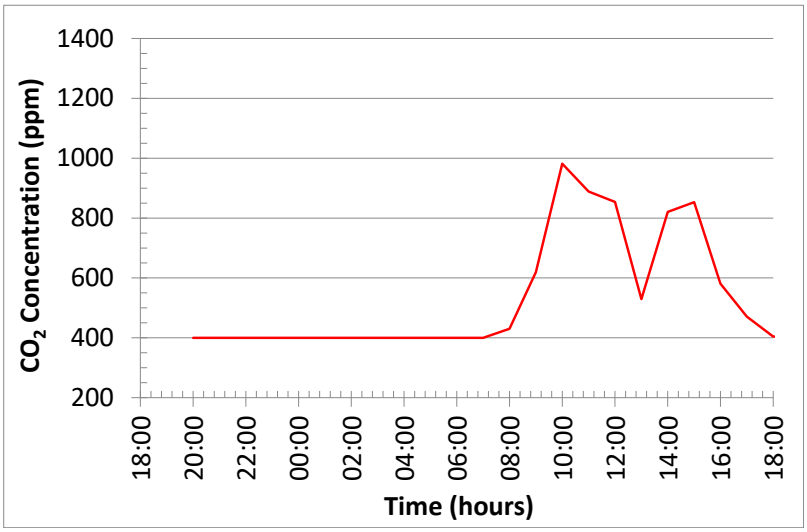

Figure 22. Simulated CO_2 concentration for the field experiment.

6. Discussion and Conclusions

The primary objective of this paper is to study and to enhance the understanding of using displacement ventilation for achieving a comfortable indoor environment in winter without the requirement of a separate heating system. As a first step towards this objective, a set of experimental tests was conducted under various realistic operating conditions. Firstly, a series of tests were performed in a scale model of a classroom under controlled laboratory conditions. It was followed by a field test in a real classroom environment with several uncontrollable disturbances influencing the operation of the system. The experimental tests were specifically aimed to assess the technical and practical suitability of the proposed concept in terms of thermal comfort, temperature stratification, and CO_2 concentration. For this purpose, the measured data can be assessed against the design criteria laid out in standard EN 16798-1 [106]. The standard specifies several categories of thermal comfort and indoor air quality and stipulates requirements for operative temperature, vertical air temperature difference between head and ankle heights, and CO_2 concentration above outdoor concentration, among others, for each category. Table 3 summarizes these requirements for various categories for classrooms.

Table 3. Design criteria for thermal comfort, temperature stratification, and CO_2 concentration according to EN 16798-1 [106].

Category	Minimum Operative Temperature for Heating (°C)	Vertical Air Temperature Difference [Seated] (K)	CO_2 Concentrations above Outdoors (ppm)
I	21	2	550
II	20	3	800
III	19	4	1350
1V	18	-	1350

The lab tests were conducted in a scale model of the classroom using two distinct scenarios. The test conditions for both scenarios were carefully controlled to simulate an

outside temperature of −15 °C. In the first scenario, the scale model of the classroom was subjected to normal operating conditions of regular occupancy and typical internal heat gains from lighting and equipment during a school day. In the second scenario, the occupancy and internal load profiles were chosen to represent an extreme case. The classroom was considered occupied only during the afternoon for three hours at half of its design occupancy and with much lower heat gains from equipment. The results of the lab tests showed that for the first scenario the operative temperatures during the occupancy periods remained 1–2 K higher than the supply temperature of 22 °C. The average and maximum temperature gradient between 0.1 and 1.1 m heights were approximately 0.7 and 1.0 K, respectively. The measured operative temperatures range under categories I of EN 16798-1, which correspond to a predicted percentage of dissatisfied (PPD) of 6%. Besides, the measured vertical temperature difference between head and ankle heights was significantly smaller than the design limit of 2 K for Category I of local thermal discomfort in EN 16798-1. For the second scenario, the operative temperature was below 21 °C at the beginning of the occupancy period but increased rapidly once the classroom was occupied. During the occupancy period, the average and maximum temperature gradient between 0.1 and 1.1 m heights were approximately 0.3, and 0.5 K, respectively. For this scenario, the measured operative temperatures ranged under categories I and II of EN 16798-1 corresponding to PPD of 6, and 10%, respectively. The measured temperature gradient between head and ankle heights was again significantly smaller than the 2 K design limit for Category I of local thermal discomfort in EN 16798-1. The occupancy and internal load profiles in the second scenario represented an extreme case. The case of no occupancy and no internal heat gains until noon, and lower than expected occupancy and internal heat gains in the afternoon, provided a stringent test of the concept under consideration.

The field test was performed in an actual classroom under real dynamic conditions of occupancy, transmission and ventilation losses, and solar gains, among others. The field test lasted for approximately 20 h, during which the displacement ventilation system was operated in the heating mode during the first 12 h and in the normal mode for the remaining time. The supply air temperature and flow to the classroom used in the normal mode represented rather extreme conditions unlikely to be encountered in actual practice. During the test period, the outdoor temperature varied between −7 and +3 °C. The number and position of heat and pollutant sources, i.e., occupants, varied frequently throughout the testing period. Solar heat gains to the classroom varied with time of day, starting around mid-morning, peaking in late morning until mid-afternoon, and declining in the late afternoon. Transmission heat losses to the ambient and the ground also varied in time, depending upon the temperature differences between inside and outside. Similarly, ventilation losses from the classroom varied in time due to changes in supply air temperature and flow, as well as due to infiltration losses from recurring door openings. The results of the field test showed that even with the rather low supply temperatures of between 16 and 18 °C, not likely to occur during the actual operation, the operative temperatures during the occupancy periods were 2–4 K higher than the supply temperature. The average and maximum temperature and CO_2 gradients between 0.1 and 1.1 m heights were approximately 0.8 and 1.1 K, and 240, and 350 ppm, respectively. The maximum average room and breathing zone CO_2 concentrations above outdoor concentration were 670 and 730 ppm, respectively. The operative temperatures measured during the occupancy periods fall under categories II and III of EN 16798-1. The lowest operative temperatures, corresponding to category III, occurred early in the morning when supply air temperatures were at their minimum and solar heat gains were absent. As in the lab tests, the measured vertical temperature difference between head and ankle heights was smaller than the 2 K design limit for category I of local thermal discomfort in EN 16798-1. The measured CO_2 concentrations in the classroom corresponded to categories I and II of recommended CO_2 concentrations above the outdoor concentration in EN 16798-2 [107].

One type of commonly used indoor air quality indicator for displacement ventilation systems is ventilation effectiveness [69,73,79,81,82]. It is the ability of the ventilation system

to exchange the air in the zone and to remove air-borne contaminants from the zone [108]. Based on the field test measurements, the ventilation effectiveness of the classroom system could be evaluated in terms of contaminant removal effectiveness and air change efficiency. The contaminant removal effectiveness, providing a measure of how quickly an airborne contaminant is removed from the zone and determined as the ratio between the steady-state concentration of CO_2 in the exhaust air and the steady-state mean concentration in the classroom, is computed to be 1.2. The air change efficiency, providing a measure of how quickly the air is replaced in the zone and calculated from concentration decay (step-down) of CO_2 during the lunch break and after the end of school when the classroom was empty, using the method described in Mundt et al. [108], was found to be between 55% and 60%. The ventilation effectiveness indices of contaminant removal effectiveness and air change efficiency are somewhat lower than reported for displacement ventilation previously, which may be attributed to differences in boundary conditions between this and earlier studies. Cold climates, such as the one investigated in this study, cause descending air flows from cold surfaces like windows and external walls, which results in a mixing of contaminated air from the upper unoccupied zone air into the lower occupied zone, thus reducing the ventilation effectiveness. A few other studies have also reported similar results, implying lower-than-normal ventilation effectiveness indices for displacement ventilation systems in cold climates [45,109]. Nevertheless, the ventilation effectiveness indices calculated from the field measurements for the classroom are still superior to the maximum possible contaminant removal effectiveness of 1 and a maximum possible air change efficiency of 50% for mixing ventilation.

The results of experimental tests clearly support the hypothesis that the proposed solution of using displacement ventilation without a separate heating system is fully capable of maintaining a comfortable indoor climate in the classroom even in peak winter periods and under extreme operating conditions. In fact, the experimental results provide answers to the questions raised in Section 3 on the application of displacement ventilation for heating during non-occupied hours. In answer to the first question, it has been found through the series of experiments that providing heating only during the non-occupied hours could be sufficient to achieve good indoor thermal comfort conditions during the occupied hours. Thermal comfort corresponding to Category I of EN 16798-1 could be achieved under typical winter operating conditions, whereas thermal comfort corresponding to Category II could be attained under extreme conditions, expected to occur only rarely in practice. In reply to the second question, it has been ascertained through the experimental tests that the vertical temperature gradient in classrooms would not be unreasonably high at the start of the school day and during the non-occupied hours. The experiments demonstrated that a temperature difference of less than 2 K between head and ankle heights, corresponding to Category I of local thermal discomfort in EN 16798-1, could be achieved during the occupancy, as well as non-occupancy periods. In relation to the third question, it has been exhibited both through the lab and field experiments that the warm air in heating mode does not ascend to the ceiling unimpeded, but rather is stratified along the height of the zone. The vertical temperature distribution in the heating mode could be noted to be a linear function of the zone height for all experimental tests. It has also been demonstrated that the warm air supplied with low impulse would indeed heat the floor and the space above. In response to the fourth question, it has been validated through Scenario II of the lab test that satisfactory thermal comfort conditions could be ensured even with exceptionally low occupancy and internal heat gains in the zone. The field test results also reaffirmed this conclusion. Finally, regarding the fifth question, while no specific experimental tests were conducted to directly analyze this issue, it could be deduced from the conducted experimental tests that satisfactory thermal comfort conditions could be achieved even if the occupancy and internal heat gains in the zone would be higher than the design values. The scenario I of the lab test showed that, under design conditions of occupancy and internal heat gains, thermal comfort in the zone could be comfortably maintained at a level corresponding to Category I of EN 16798-1. Although, the greater-than-design levels

of occupancy and internal loads would increase the operative temperatures and vertical temperature gradient in the zone, but an increase beyond the threshold levels of 25 °C for operative temperature and 3 K for temperature gradient between the head and ankle heights, corresponding to Category II of thermal comfort in EN 16798-1, would be unlikely. Moreover, it has been demonstrated through the field test that in case of greater-than-design levels of occupancy and internal loads, supply temperatures in heating mode could be lowered to maintain satisfactory thermal comfort conditions in the zone.

As a second step towards realizing the research objective, numerical simulations of experimental tests were carried out using a state-of-the-art building indoor climate simulation program. The purpose of this step was to assess whether numerical simulations and state-of-the-art modeling methods are capable of accurately capturing experimentally observed temperature and CO_2 distributions for the proposed concept. The results of numerical simulation of the lab tests showed that for the first scenario the simulated average and maximum temperature difference between head and ankle heights during the occupancy periods was 0.3, and 0.5, respectively. The simulated temperature gradient between head and ankle heights was zero during the non-occupancy periods, except for lunch breaks when internal loads from lighting and equipment were still present. For the occupancy periods, the simulated temperature gradients between head and ankle heights are only half of the experimental values. This is despite a very good match between the simulated and experimentally measured temperature gradients from floor to ceiling. This can be attributed to the stratification model used by the simulation program. The model has certain limitations, in terms of accurately modeling temperature stratification in the zone, as well as identifying the stratification height in the space, as previously suggested by other researchers, including Mateus and da Graça [30] and Lastovets et al. [110], among others. For the non-occupancy period, numerical simulations were unable to provide a good estimate of temperature gradient that can be compared to the experimental data. The numerical simulations were also unable to calculate the temperature stratification for both the occupancy, as well as the non-occupancy periods of the second scenario and were consequently not able to replicate the thermal gradients observed experimentally in the lab test.

The results of the numerical simulation of the field test showed that the simulated average and maximum temperature difference between head and ankle heights during the occupancy periods was 0.9, and 1.1, respectively. During the non-occupancy period, the temperature gradient was simulated to be zero. The temperature gradients simulated between head and ankle heights for the occupancy periods were quite similar to the experimental values. However, there was a pronounced mismatch between the simulated and experimentally measured temperature gradients from floor to ceiling, with simulations overestimating the temperature gradients by a factor of over two. The simulated vertical temperature gradient was modeled to be linear over the classroom height, while the experimentally measured temperature gradient was observed to be non-linear. In point of fact, the measured temperature and contaminant distribution in the classroom indicated that space was divided into two distinct zones separated by a stratification height. Below the stratification height, the air temperature increased with height, whereas, above the stratification height, there existed a small negative temperature gradient. The stratification height was not evident in the simulated vertical temperature profile. As in the case of lab tests, the numerical simulations could not predict the temperature gradients observed in the field test during the non-occupancy period. Numerical simulations also could not compute the vertical CO_2 concentration gradients due to the model limitations and could only predict the mean CO_2 stratification. The simulated mean CO_2 concentrations were slightly lower than the average CO_2 levels measured experimentally. This could be because the numerical simulations used a constant rate of CO_2 generation for each occupant throughout the day. In reality, the CO_2 generation rate per occupant could vary widely based upon factors, such as occupant's activity level, metabolic rate, and body surface area, among others [111].

It is evident from the above discussion that the results of numerical simulations are inconsistent with the experimental results. The numerical simulations completely failed to predict the vertical temperature profiles when providing heating through displacement ventilation. The numerical simulations also could not correctly capture the experimental results in the normal mode when the supply air temperature was lower than the space temperature. This was even though the numerical simulations were carried out with great care and attention to detail to match the experimental conditions as closely as possible. The discrepancies between experimental and numerical results are relatively large and could not be explained by experimental uncertainties of temperature measurements that did not exceed ± 0.2 and ± 0.5 K for lab, and field tests, respectively. Therefore, other factors related to the experimental tests and/or the numerical analysis must be responsible for the differences in experimental and numerical results observed in this study.

Some of the discrepancies between experimental tests and simulation results might be attributed to uncertainties and limitations associated with the analysis, particularly with regard to the simulation of dynamic conditions during the tests. For instance, the type and location of heat sources, such as occupants, equipment, and lights in numerical simulations were considered not to influence the temperature stratification in the zone. Heat gains from these sources were taken to be evenly distributed over the zone volume and zone surfaces. As a matter of fact, both the type and location of heat sources have a significant impact on the temperature stratification in the zone [10,60–63]. Moreover, while significant stochastic movements of occupants inside the classroom were observed during the field test, numerical simulations of the field test could not account for the occupant movement within the classroom. Previous research shows that movements in a zone with displacement ventilation can substantially affect the stratification in the zone [65,112,113]. Similarly, although, the volumetric exchange of air due to the combined effect of natural convection and forced airflow through the classroom door was implicitly included in the calculation of infiltration losses, the effect of classroom door openings on the temperature stratification could not be explicitly accounted for in the numerical simulations. Some earlier studies have shown that door openings may influence the airflow pattern in rooms with displacement ventilation [66,72].

Moreover, another factor contributing to the discrepancy between the field test and simulation might be the assumptions and simplifications made in developing the computational model of the classroom. First of all, the geometry of the classroom was simplified to a rectangular footprint in the computational model. Second, there was some level of uncertainty associated with estimating the heat loss to the ground. This was because the field test was performed just after the completion of the building when the concrete slab had not dried out completely. Next, the effects of external shading from terrain and vegetation were approximated based on visual observations on the day of the field test. Finally, simulation inputs of direct and diffused components of solar radiation were approximated from global radiation measurements over the test period from a nearby weather station.

Future work regarding this research should seek to repeat the numerical simulations of experimental tests using more-sophisticated nodal models, such as those proposed by Nielsen [29] and Mateus and da Graça [30]. At present, the implementation of these models in building performance simulation programs is largely lacking. Future work should also focus on advanced transient CFD simulations of experimental tests using actual zone geometries and design inputs matching experimental conditions. The future simulations should allow for a more precise analysis of displacement ventilation by capturing the non-linear vertical temperature distribution in the zone, by determining the stratification height, and by accounting for heat exchange between the space and the surrounding surfaces in a more comprehensive manner. These simulations are also expected to describe the thermal stratification in the heating mode more accurately, and thus, provide a better match with experimental results for heating the classroom through displacement ventilation. More broadly, future work should further develop the idea of providing heating through displacement ventilation only. It should also include finding general rules of

thumb regarding vertical temperature distribution in the zone when heating the zone with displacement ventilation.

To conclude, this study was designed to explore whether displacement ventilation could be used for preheating a space outside occupancy periods to provide an acceptable indoor climate during the occupancy periods without utilizing any separate heating system. In exploring this concept, a series of experimental tests were performed in laboratory and field settings, under conditions ranging from normal to extreme. Extensive measurements were made to characterize the temperature and CO_2 distributions during the tests. Numerical simulations of the experimental tests were performed to assess the suitability of a state-of-the-art building performance evaluation program that incorporates a commonly used temperature stratification model for predicting the design and performance of the proposed concept. The experimental results clearly demonstrated that the proposed concept of using displacement ventilation without a separate heating system is fully capable of maintaining a comfortable indoor climate even in peak winter periods and under extreme operating conditions. The results of numerical simulations suggested that existing design tools with simplistic stratification models are incapable of capturing the thermal behavior and actual performance of the proposed concept. Advanced numerical simulations utilizing detailed stratification models and taking into account actual geometry and layout of the zone, and the transient aspects of the system would be a more effective way of analysis.

Author Contributions: S.J.: Conceptualization (equal); data curation (lead); formal analysis (lead); funding acquisition (supporting); investigation (equal); methodology (equal); project administration (equal); resources (equal); software (supporting); validation (lead); visualization (lead); writing–original draft (lead); writing–review and editing (lead). I.R.Ø.: formal analysis (supporting); investigation (equal); methodology (equal); resources (equal); software (lead); validation (supporting); visualization (supporting); writing–original draft (supporting); writing–review and editing (supporting). T.H.D.: conceptualization (equal); funding acquisition (lead); investigation (equal); methodology (equal); project administration (equal); resources (equal); validation (supporting); writing–original draft (supporting); writing–review and editing (supporting). M.M.: data curation (supporting); formal analysis (supporting); investigation (equal); methodology (equal); resources (equal); visualization (supporting). S.B.H.: data curation (supporting); formal analysis (supporting); investigation (equal); methodology (equal); resources (equal). All authors have read and agreed to the published version of the manuscript.

Funding: The research reported in this article was partly funded by the Research Council of Norway (Norges Forskningsråd) national program ENERGIX through research grants LowEx (269705) and SynHouse (310121).

Institutional Review Board Statement: Not applicable.

Informed Consent Statement: Not applicable.

Data Availability Statement: The data presented in this study are available on request from the corresponding author.

Acknowledgments: The authors acknowledge the support offered by Drøbak Montessori school.

Conflicts of Interest: The authors declare no conflict of interest. The funding source had no involvement in the study design; the collection, analysis, and interpretation of data; or in the decision to submit the article for publication.

References

1. Zhang, J. Integrating IAQ control strategies to reduce the risk of asymptomatic SARS CoV-2 infections in classrooms and open plan offices. *Sci. Technol. Built Environ.* **2020**, *26*, 1013–1018. [CrossRef]
2. Dorgan, C.B.; Dorgan, C.E.; Kanarek, M.S.; Willman, A.J. Health and productivity benefits of improved indoor air quality. *Ashrae Trans.* **1998**, *104*, 658–666.
3. Šujanová, P.; Rychtáriková, M.; Sotto Mayor, T.; Hyder, A. A healthy, energy-efficient and comfortable indoor environment, a review. *Energies* **2019**, *12*, 1414. [CrossRef]
4. Maroni, M.; Seifert, B.; Lindvall, T. *Indoor Air Quality: A Comprehensive Reference Book*; Elsevier: Amsterdam, The Netherlands, 1995.

5. Santos, H.R.; Leal, V.M. Energy vs. ventilation rate in buildings: A comprehensive scenario-based assessment in the European context. *Energy Build.* **2012**, *54*, 111–121. [CrossRef]
6. BRE. *BREEAM International New Construction 2016*; Building Research Establishment: Watford, UK, 2016.
7. USGBC. *LEED v4.1 Building Design and Construction*; Green Building Council: Washington, DC, USA, 2020.
8. ASHRAE. *Ventilation for Acceptable Indoor Air Quality (ASHRAE Standard 62.1-2016)*; American Society of Heating, Refrigerating, and Air-Conditioning Engineers, Inc.: Atlanta, GA, USA, 2016.
9. Kosonen, R.; Melikov, A.; Mundt, E.; Mustakallio, P.; Nielsen, P.V. *REHVA Guidebook, No. 23: Displacement Ventilation*; REHVA: Brussels, Belgium, 2017.
10. Causone, F.; Olesen, B.W.; Corgnati, S.P. Floor heating with displacement ventilation: An experimental and numerical analysis. *HvacR Res.* **2010**, *16*, 139–160. [CrossRef]
11. Martinopoulos, G.; Papakostas, K.T.; Papadopoulos, A.M. A comparative review of heating systems in EU countries, based on efficiency and fuel cost. *Renew. Sustain. Energy Rev.* **2018**, *90*, 687–699. [CrossRef]
12. de Klijn-Chevalerias, M.; Javed, S. The Dutch approach for assessing and reducing environmental impacts of building materials. *Build. Environ.* **2017**, *111*, 147–159. [CrossRef]
13. Jiang, Z.; Chen, Q.; Lee, K. *Air Distribution Effectiveness With Stratified Air Distribution Systems*; Final Report for ASHRAE RP-1373; ASHRAE: Atlanta, GA, USA, 2009.
14. Ouazia, B.; Thompson, A.; Macdonald, I.; Booth, D.; Tardif, M. Contaminant Removal Effectiveness of Displacement Ventilation Systems During Heating Season; Summary Results from Three Field Studies. *Ashrae Trans.* **2012**, *118*, 292–299.
15. Halton Inc. *Displacement Ventilation Design Guide*; Halton Oy: Helsinki, Finland, 2000.
16. Price Industries. Fundamentals of Displacement Ventilation. In *Price Engineer's HVAC Handbook–A Comprehensive Guide to HVAC Fundamentals*; Price Industries Limited: Winnipeg, MB, Canada, 2011.
17. Skistad, H.; Mundt, E.; Nielsen, P.V.; Hagström, K.; Railio, J. *REHVA Guidebook No. 1: Displacement Ventilation in Non-Industrial Premises*; REHVA: Brussels, Belgium, 2002.
18. Chen, Q.; Glicksman, L. *System Performance Evaluation and Design Guidelines for Displacement Ventilation*; American Society of Heating, Refrigerating, and Air-Conditioning Engineers, Inc.: Atlanta, GA, USA, 2003.
19. AEC. *Displacement Ventilation Design Guide: K-12 Schools. Final Report for Public Interest Energy Research Program, California Energy Commission*; Architectural Energy Corporation: Sacramento, CA, USA, 2006.
20. Scheff, P.A.; Paulius, V.K.; Huang, S.W.; Conroy, L.M. Indoor air quality in a middle school, Part I: Use of CO2 as a tracer for effective ventilation. *Appl. Occup. Environ. Hyg.* **2000**, *15*, 824–834. [CrossRef]
21. de Gennaro, G.; Dambruoso, P.R.; Loiotile, A.D.; Di Gilio, A.; Giungato, P.; Tutino, M.; Marzocca, A.; Mazzone, A.; Palmisani, J.; Porcelli, F. Indoor air quality in schools. *Environ. Chem. Lett.* **2014**, *12*, 467–482. [CrossRef]
22. Jovanović, M.; Vučićević, B.; Turanjanin, V.; Živković, M.; Spasojević, V. Investigation of indoor and outdoor air quality of the classrooms at a school in Serbia. *Energy* **2014**, *77*, 42–48.
23. Congedo, P.M.; D'Agostino, D.; Baglivo, C.; Tornese, G.; Zacà, I. Efficient solutions and cost-optimal analysis for existing school buildings. *Energies* **2016**, *9*, 851. [CrossRef]
24. Fisk, W.J. The ventilation problem in schools: Literature review. *Indoor Air* **2017**, *27*, 1039–1051. [CrossRef]
25. Daisey, J.M.; Angell, W.J.; Apte, M.G. Indoor air quality, ventilation and health symptoms in schools: An analysis of existing information. *Indoor Air* **2003**, *13*, 53–64. [CrossRef]
26. Norbäck, D.; Wieslander, G.; Zhang, X.; Zhao, Z. Respiratory symptoms, perceived air quality and physiological signs in elementary school pupils in relation to displacement and mixing ventilation system: An intervention study. *Indoor Air* **2011**, *21*, 427–437. [CrossRef] [PubMed]
27. Holland, D.; Livchak, A. Improving indoor air quality in schools by utilizing displacement ventilation system. *Proc. Indoor Air* **2002**, *4*, 278–282.
28. Mundt, E. The Performance of Displacement Ventilation Systems-Experimental and Theoretical Studies. Ph.D. Thesis, Royal Institute of Technology (KTH), Stockholm, Sweden, 1996.
29. Nielsen, P.V. Temperature and Air Velocity Distribution in Rooms Ventilated by Displacement Ventilation. In Proceedings of the 7th International Symposium on Ventilation for Contaminant Control (Ventilation 2003), Sapporo, Japan, 5–8 August 2003.
30. Mateus, N.M.; da Graça, G.C. A validated three-node model for displacement ventilation. *Build. Environ.* **2015**, *84*, 50–59. [CrossRef]
31. DOE. *"EnergyPlus."*; Version 9.2.0; US Department of Energy: Washington, DC, USA, 2019; [Computer Software].
32. EQUA. *"IDA Indoor Climate and Energy"*; Version 4.8; Simulations AB: Stockholm, Sweden, 2018; [Computer Software].
33. Skåret, E. *Ventilasjonsteknikk*; Institute of Heating, Ventilation and Sanitary Techniques: Trondheim, Norway, 1986. Textbook (In Norwegian)
34. Koganei, M.; Holbrook, G.T.; Olesen, B.W.; Woods, J.E. Modeling the Thermal and Indoor Air Quality Performance of the Vertical Displacement Ventilation Systems. *Indoor Air* **1993**, *93*, 241–246.
35. Sandberg, E.; Koskela, H.; Hautalampi, T. Convective Flows and Vertical Temperature Gradient with the Active Displacement Air Distribution. In Proceedings of the Roomvent 98: 6th International Conference on Air Distribution in Rooms, Stockholm, Sweden, 14–17 June 1998.

36. Dokka, T.H. Modelling of Indoor Air Quality in Residential and Commercial Buildings. Ph.D. Thesis, Norwegian University of Science and Technology (NTNU), Trondheim, Norway, 2020.
37. Yamanaka, T.; Kotani, H.; Xu, M. Zonal Models to Predict Vertical Contaminant Distribution in Room with Displacement Ventilation Accounting for Convection Flows Along Walls. In Proceedings of the Roomvent–10th International Conference on Air Distribution in Rooms, Helsinki, Finland, 13–15 June 2007; FINVAC; FINVAC.
38. Okutan, G.M. Scale Model Studies of Displacement Ventilation. Bachelor's Thesis, Massachusetts Institute of Technology, Cambridge, MA, USA, 1995.
39. Brohus, H.; Nielsen, P.V. Contaminant Distribution Around Persons in Rooms Ventilated by Displacement Ventilation. In Proceedings of the ROOMVENT '94, Fourth International Conference on Air Distribution in Rooms, Cracow, Poland, 15–17 June 1994.
40. Brohus, H.; Nielsen, P.V. Personal exposure in displacement ventilated rooms. *Indoor Air* **1996**, *6*, 157–167. [CrossRef]
41. Akimoto, T.; Nakano, J.; Tanabe, S.; Kimura, K. Experimental study on indoor thermal environment of floor-supply displacement ventilation system under various heat load conditions. *J. Archit. Plan.* **1998**, *63*, 27–34. [CrossRef]
42. Yuan, X.; Chen, Q.; Glicksman, L.R. Performance evaluation and design guidelines for displacement ventilation. *Ashrae Trans.* **1999**, *105*, 298.
43. Yuan, X.; Chen, Q.; Glicksman, L.R.; Hu, Y.; Yang, X. Measurements and computations of room airflow with displacement ventilation. *Ashrae Trans.* **1999**, *105*, 340.
44. Xu, M.; Yamanaka, T.; Kotani, H.; Higashimoto, T. Effect of cooled or heated wall on vertical distribution of temperature and contaminant concentration in rooms with displacement ventilation. *J. Archit. Plan. Environ. Eng.* **2001**, *544*, 17–23.
45. Xu, M.; Yamanaka, T.; Kotani, H. Vertical profiles of temperature and contaminant concentration in rooms ventilated by displacement with heat loss through room envelopes. *Indoor Air* **2001**, *11*, 111–119. [CrossRef]
46. Mundt, E. Non-buoyant pollutant sources and particles in displacement ventilation. *Build. Environ.* **2001**, *36*, 829–836. [CrossRef]
47. Cheong, K.W.D.; Yu, W.J.; Kosonen, R.; Tham, K.W.; Sekhar, S.C. Assessment of thermal environment using a thermal manikin in a field environment chamber served by displacement ventilation system. *Build. Environ.* **2006**, *41*, 1661–1670. [CrossRef]
48. Cheong, K.W.D.; Yu, W.J.; Sekhar, S.C.; Tham, K.W.; Kosonen, R. Local thermal sensation and comfort study in a field environment chamber served by displacement ventilation system in the tropics. *Build. Environ.* **2007**, *42*, 525–533. [CrossRef]
49. Wachenfeldt, B.J.; Mysen, M.; Schild, P.G. Air flow rates and energy saving potential in schools with demand-controlled displacement ventilation. *Energy Build.* **2007**, *39*, 1073–1079. [CrossRef]
50. Trzeciakiewicz, Z. An experimental analysis of the two-zone airflow Pattern Formed in a room with displacement ventilation. *Int. J. Vent.* **2008**, *7*, 221–231. [CrossRef]
51. Yu, W.J.; Cheong, K.W.D.; Tham, K.W.; Sekhar, S.C.; Kosonen, R. Thermal effect of temperature gradient in a field environment chamber served by displacement ventilation system in the tropics. *Build. Environ.* **2007**, *42*, 516–524. [CrossRef]
52. Lin, Z.; Chow, T.T.; Tsang, C.F.; Chan, L.S.; Fong, K.F. Effect of air supply temperature on the performance of displacement ventilation (Part I)-thermal comfort. *Indoor Built Environ.* **2005**, *14*, 103–115. [CrossRef]
53. Lin, Z.; Chow, T.T.; Tsang, C.F.; Fong, K.F.; Chan, L.S. CFD study on effect of the air supply location on the performance of the displacement ventilation system. *Build. Environ.* **2005**, *40*, 1051–1067. [CrossRef]
54. Kang, Y.; Wang, Y.; Zhong, K. Effects of supply air temperature and inlet location on particle dispersion in displacement ventilation rooms. *Particuology* **2011**, *9*, 619–625. [CrossRef]
55. Kobayashi, N.; Chen, Q. Floor-supply displacement ventilation in a small office. *Indoor Built Environ.* **2003**, *12*, 281–291. [CrossRef]
56. Lin, Y.J.P.; Lin, C.L. A study on flow stratification in a space using displacement ventilation. *Int. J. Heat Mass Transf.* **2014**, *73*, 67–75. [CrossRef]
57. Mathisen, H.M. Displacement ventilation-the influence of the characteristics of the supply air terminal device on the airflow pattern. *Indoor Air* **1991**, *1*, 47–64. [CrossRef]
58. Zhang, T.; Lee, K.; Chen, Q. A simplified approach to describe complex diffusers in displacement ventilation for CFD simulations. *Indoor Air* **2009**, *19*, 255–267. [CrossRef]
59. Cehlin, M.; Moshfegh, B. Numerical modeling of a complex diffuser in a room with displacement ventilation. *Build. Environ.* **2010**, *45*, 2240–2252. [CrossRef]
60. Park, H.J.; Holland, D. The effect of location of a convective heat source on displacement ventilation: CFD study. *Build. Environ.* **2001**, *36*, 883–889. [CrossRef]
61. Rees, S.J.; McGuirk, J.J.; Haves, P. Numerical investigation of transient buoyant flow in a room with a displacement ventilation and chilled ceiling system. *Int. J. Heat Mass Transf.* **2001**, *44*, 3067–3080. [CrossRef]
62. Deevy, M.; Sinai, Y.; Everitt, P.; Voigt, L.; Gobeau, N. Modelling the effect of an occupant on displacement ventilation with computational fluid dynamics. *Energy Build.* **2008**, *40*, 255–264. [CrossRef]
63. Zhong, K.; Kang, Y.; Wang, Y. Effect of source location on particle dispersion in displacement ventilation rooms. *Particuology* **2008**, *6*, 362–368. [CrossRef]
64. Matsumoto, H.; Matsusaki, A.; Ohba, Y. CFD Simulation of Air Distribution in Displacement Ventilated Rooms with a Moving Object. In Proceedings of the Roomvent Congress, University of Coimbra, Coimbra, Portugal, 5–8 September 2004.
65. Matsumoto, H.; Ohba, Y. The influence of a moving object on air distribution in displacement ventilated rooms. *J. Asian Archit. Build. Eng.* **2004**, *3*, 71–75. [CrossRef]

66. Mazumdar, S.; Yin, Y.; Guity, A.; Marmion, P.; Gulick, B.; Chen, Q. Impact of Moving Objects on Contaminant Concentration Distributions in an Inpatient Ward with Displacement Ventilation. *HvacR Res.* **2010**, *16*, 545–563. [CrossRef]
67. Li, Y.; Fuchs, L.; Sandberg, M. Numerical prediction of airflow and heat-radiation interaction in a room with displacement ventilation. *Energy Build.* **1993**, *20*, 27–43. [CrossRef]
68. Faure, X.; Le Roux, N. Time dependent flows in displacement ventilation considering the volume envelope heat transfers. *Build. Environ.* **2012**, *50*, 221–230. [CrossRef]
69. Wu, X.; Olesen, B.W.; Fang, L.; Zhao, J. A nodal model to predict vertical temperature distribution in a room with floor heating and displacement ventilation. *Build. Environ.* **2013**, *59*, 626–634. [CrossRef]
70. Lin, Z.; Chow, T.T.; Tsang, C.F.; Fong, K.F.; Chan, L.S. Effects of headroom on the performance of the displacement ventilation system. *Indoor Built Environ.* **2006**, *15*, 333–346. [CrossRef]
71. Hashimoto, Y.; Yoneda, H. Numerical Study on the Influence of a Ceiling Height for Displacement Ventilation. In Proceedings of the 11th International IBPSA Conference, Glasgow, Scotland, UK, 27–30 July 2009.
72. Lin, Z.; Chow, T.T.; Tsang, C.F. Effect of door opening on the performance of displacement ventilation in a typical office building. *Build. Environ.* **2007**, *42*, 1335–1347. [CrossRef]
73. Xing, H.; Hatton, A.; Awbi, H.B. A study of the air quality in the breathing zone in a room with displacement ventilation. *Build. Environ.* **2001**, *36*, 809–820. [CrossRef]
74. Xing, H.; Awbi, H.B. Measurement and calculation of the neutral height in a room with displacement ventilation. *Build. Environ.* **2002**, *37*, 961–967. [CrossRef]
75. Lau, J.; Chen, Q. Floor-supply displacement ventilation for workshops. *Build. Environ.* **2007**, *42*, 1718–1730. [CrossRef]
76. Fatemi, I.; Wang, B.C.; Koupriyanov, M.; Tully, B. Experimental study of a non-isothermal wall jet issued by a displacement ventilation system. *Build. Environ.* **2013**, *66*, 131–140. [CrossRef]
77. Fernández-Gutiérrez, A.; González-Prieto, I.; Parras, L.; Gutiérrez-Castillo, P.; Cejudo-López, J.M.; del Pino, C. Experimental and numerical study of a small-scale and low-velocity indoor diffuser for displacement ventilation: Isothermal floor. *Appl. Therm. Eng.* **2015**, *87*, 79–88. [CrossRef]
78. Magnier-Bergeron, L. Measurement, Analysis, and Modeling of Non-Isothermal Low-Velocity Displacement Ventilation Jets. Bachelor's Thesis, Concordia University Montreal, Quebec, QC, Canada, 2015.
79. Causone, F.; Baldin, F.; Olesen, B.W.; Corgnati, S.P. Floor heating and cooling combined with displacement ventilation: Possibilities and limitations. *Energy Build.* **2010**, *42*, 2338–2352. [CrossRef]
80. Rees, S.J.; Haves, P. An experimental study of air flow and temperature distribution in a room with displacement ventilation and a chilled ceiling. *Build. Environ.* **2013**, *59*, 358–368. [CrossRef]
81. Schiavon, S.; Bauman, F.S.; Tully, B.; Rimmer, J. Chilled ceiling and displacement ventilation system: Laboratory study with high cooling load. *Sci. Technol. Built Environ.* **2015**, *21*, 944–956. [CrossRef]
82. Ouazia, B.; Tardif, M.; Macdonald, I.; Thompson, A.; Booth, D. In-situ performance of displacement ventilation system in Canadian schools with radiant heating systems. *Ashrae Trans.* **2011**, *117*, 207–220.
83. Akimoto, T.; Nobe, T.; Tanabe, S.; Kimura, K. Experimental Study on Indoor Thermal Environment and Ventilation Performance of Floor-Supply Displacement Ventilation System. *J. Archit. Plan.* **1997**, *62*, 17–25. [CrossRef]
84. Rimmer, J.; Tully, B.; Guity, A. A Field Study of the Air Change Effectiveness of Overhead Air Distribution and Displacement Ventilation in Healthcare. Proceedings of IAQ 2010, Kuala Lumpur, Malaysia, 10–12 November 2010.
85. Breum, N.O. Ventilation efficiency in an occupied office with displacement ventilation—A laboratory study. *Environ. Int.* **1992**, *18*, 353–361. [CrossRef]
86. Olmedo, I.; Nielsen, P.V.; Ruiz de Adana, M.; Jensen, R.L.; Grzelecki, P. Distribution of exhaled contaminants and personal exposure in a room using three different air distribution strategies. *Indoor Air* **2012**, *22*, 64–76. [CrossRef]
87. Wu, X.; Fang, L.; Olesen, B.W.; Zhao, J.; Wang, F. Air distribution in a multi-occupant room with mixing or displacement ventilation with or without floor or ceiling heating. *Sci. Technol. Built Environ.* **2015**, *21*, 1109–1116. [CrossRef]
88. Behne, M. Indoor air quality in rooms with cooled ceilings.: Mixing ventilation or rather displacement ventilation? *Energy Build.* **1999**, *30*, 155–166. [CrossRef]
89. Cermak, R.; Melikov, A.K.; Forejt, L.; Kovar, O. Performance of personalized ventilation in conjunction with mixing and displacement ventilation. *HvacR Res.* **2006**, *12*, 295–311. [CrossRef]
90. Cermak, R.; Melikov, A.K. Air quality and thermal comfort in an office with underfloor, mixing and displacement ventilation. *Int. J. Vent.* **2006**, *5*, 323–352. [CrossRef]
91. Yin, Y.; Xu, W.; Gupta, J.K.; Guity, A.; Marmion, P.; Manning, A.; Gulick, B.; Zhang, X.; Chen, Q. Experimental study on displacement and mixing ventilation systems for a patient ward. *HvacR Res.* **2009**, *15*, 1175–1191. [CrossRef]
92. Smedje, G.; Mattsson, M.; Wålinder, R. Comparing mixing and displacement ventilation in classrooms: Pupils' perception and health. *Indoor Air* **2011**, *21*, 454–461. [CrossRef]
93. Hu, S.; Chen, Q.; Glicksman, L.R. Comparison of energy consumption between displacement and mixing ventilation systems for different US buildings and climates. *Ashrae Trans.* **1999**, *105*, 453.
94. Lin, Z.; Chow, T.T.; Fong, K.F.; Wang, Q.; Li, Y. Comparison of performances of displacement and mixing ventilations. *Part I Thermal Comfort. Int. J. Refrig.* **2005**, *28*, 276–287. [CrossRef]

95. Lin, Z.; Chow, T.T.; Fong, K.F.; Tsang, C.F.; Wang, Q. Comparison of performances of displacement and mixing ventilations. *Part II Indoor Air Quality. Int. J. Refrig.* **2005**, *28*, 288–305.
96. ENOVA. *Enovas Byggstatistikk 2017 (in Norwegian)*; ENOVA SF: Trondheim, Norway, 2018.
97. Georges, L.; Berner, M.; Mathisen, H.M. Air heating of passive houses in cold climates: Investigation using detailed dynamic simulations. *Build. Environ.* **2014**, *74*, 1–12. [CrossRef]
98. Standard Norge. *NS 3701: Kriterier for Passivhus Og Lavenergibygninger–Yrkesbygninger (Criteria for Passive Houses and Low Energy Buildings Non-Residential Buildings)*; Standard Norge: Oslo, Norway, 2012.
99. Feist, W.; Schnieders, J.; Dorer, V.; and Haas, A. Re-inventing air heating: Convenient and comfortable within the frame of the Passive House concept. *Energy Build.* **2005**, *37*, 1186–1203. [CrossRef]
100. Cablé, A.; Mysen, M.; Thunshelle, K. Can Demand-Controlled Ventilation replace space heating in buildings with low-energy demand? In Proceedings of the Indoor Air 2014, Hong-Kong, 7–12 July 2014.
101. Powerhouse. Powerhouse Drøbak Montessori School, 2020. Available online: https://www.powerhouse.no/en/prosjekter/powerhouse-drobak-montesorri/ (accessed on 27 November 2020).
102. Abugabbara, M.; Javed, S. Validation of TEKNOsim 6 According to CIBSE TM33. In *Cold Climate HVAC Conference*; Springer: Cham, Switzerland, 2018; pp. 665–676.
103. CEN. *EN 15265:2007: Energy Performance of Buildings–Calculation of Energy Needs for Space Heating and Cooling Using Dynamic Methods–General Criteria and Validation Procedures*; CEN–European Committee for Standardization: Brussels, Belgium, 2007.
104. ASHRAE. *ASHRAE Standard 140-2014: Standard Method of Test for the Evaluation of Building Energy Analysis Computer Programs*; American Society of Heating, Refrigerating, and Air-Conditioning Engineers, Inc.: Atlanta, GA, USA, 2014.
105. CEN. *EN ISO 7726:2001: Ergonomics of the Thermal Environment-Instruments for Measuring Physical Quantities*; CEN–European Committee for Standardization: Brussels, Belgium, 2001.
106. CEN. *EN 16798-1:2019: Energy Performance of Buildings–Part 1: Indoor Environmental Input Parameters for Design and Assessment of Energy Performance of Buildings Addressing Indoor Air Quality, Thermal Environment, Lighting and Acoustics*; CEN–European Committee for Standardization: Brussels, Belgium, 2019.
107. CEN. *EN 16798-2:2019: Energy Performance of Buildings–Part 2: Indoor Environmental Input Parameters for Design and Assessment of Energy Performance of Buildings Addressing Indoor Air Quality, Thermal Environment, Lighting and Acoustics—Interpretation of the Requirements in EN 16798–1*; CEN—European Committee for Standardization: Brussels, Belgium, 2019.
108. Mundt, E.; Mathisen, H.M.; Nielsen, P.V.; Moser, A. *REHVA Guidebook, No. 2: Ventilation Effectiveness*; REHVA: Brussels, Belgium, 2004.
109. Hansson, P.; Stymne, H. A Technique to Improve the Performance of Displacement Ventilation During Cold Climate Conditions. In Proceedings of the 17th AIVC Conference, Gothenburg, Sweden, 17–20 September 1996.
110. Lastovets, N.; Kosonen, R.; Jokisalo, J. The comparison of design airflow rates with dynamic and steady-state displacement models in varied dynamic conditions. *Build. Simul.* **2020**. [CrossRef]
111. ASHRAE. *ASHRAE Handbook: Fundamentals 2017*; American Society of Heating, Refrigerating, and Air-Conditioning Engineers, Inc.: Atlanta, GA, USA, 2017.
112. Sandberg, M.; Mattsson, M. The Effect of Moving Heat Sources Upon the Stratification in Rooms Ventilated by Displacement Ventilation. In Proceedings of the 3rd International Conference on Air Distribution in Rooms (ROOMENT 92), Aalborg, Denmark, 2–4 September 1992.
113. Brohus, H.; Balling, K.D.; Jeppesen, D. Influence of movements on contaminant transport in an operating room. *Indoor Air* **2006**, *16*, 356–372. [CrossRef] [PubMed]